C.P. No. 1380

C.P. No. 1380

PROCUREMENT EXECUTIVE, MINISTRY OF DEFENCE

AERONAUTICAL RESEARCH COUNCIL

CURRENT PAPERS

The Strength of Bolted Joints in Multi-Directional CFRP Laminates

by

T. A. Collings

Structures Dept., R.A.E., Farnborough Hants

LONDON: HER MAJESTY'S STATIONERY OFFICE

1977

£3-00 NET

Editor's Note

The series of Current Papers (CP) of the Aeronautical Research Council will shortly be discontinued.

The series of Reports and Memoranda (R&M) will continue to be published. Some papers which would otherwise have appeared in the CP Series will be published as R&Ms.

UDC 621.882 : 661.66-426 : 678.046 : 621-419 : 539.41

*CP No.1380
December 1975

THE STRENGTH OF BOLTED JOINTS IN MULTI-DIRECTIONAL CFRP LAMINATES

by

T. A. Collings

SUMMARY

Tests have been carried out on simple bolted joints in multi-directional CFRP for a range of laminate configurations and hole sizes. For single-hole joints the various modes of failure have been isolated and the corresponding strengths measured; the effects of variables such as ply orientation, laminate thickness and bolt clamping pressure are discussed in the light of the results.

Multi-hole joints have been designed using the single-hole data and test results show that for normal bolt spacings there is little interaction between holes. The results also show that the specific static strengths of these joints can be significantly better than those in conventional materials such as aluminium alloy and steel.

---

* Replaces RAE Technical Report 75127 - ARC 36968

CONTENTS

1 INTRODUCTION

Perhaps the most successful applications of fibre reinforced plastics to highly stressed structures over the past decade have been in filament wound components such as pressure vessels and rocket motor casings (see for example Refs.1-3), due at least in part to the absence of any significant attachment or jointing problems. More recently several successful aircraft structural components[4-10] have been made using carbon or boron fibre preimpregnated sheet or tape and these were generally chosen to avoid severe jointing problems. However, the design and testing of these components, together with some theoretical and experimental work on specific types of joint[11-14], have shown that an ability to join elements together efficiently in terms of both minimum weight and minimum cost is central to a full exploitation of high performance fibre reinforced plastics.

It is for these reasons that several potential jointing techniques have been the subject of recent investigation in both the UK[15-17] and the USA[14,18-20], and of these adhesive bonded joints and multi-shim joints have probably received most attention to date. The simple bonded joint is attractive for two main reasons; it is simple to fabricate and stress concentrations arising from discontinuities, such as are found in mechanical joints, are largely eliminated. However, even with the use of advanced adhesives, several adverse features are to be found in bonded joints. Only relatively low rates of load transfer can be realised due to the correspondingly low shear strengths of both the adhesive and the laminated composite, high thermal strains can exist in the bonded region due to the relatively high cure temperatures of adhesives, and degradation of adhesive properties often occurs after exposure to certain environments. The multi-shim joint, using thin metal shims interleaved with the composite layers, is a compromise between bonded joints and mechanical joints and attempts to use the advantages found in each. But with an increasing emphasis on overall cost reduction and therefore on fabricational simplicity, the use of shims is no longer such an attractive technique.

By contrast, the use of simple bolted joints for composites, particularly CFRP, has received little attention, although some work on both boron and carbon fibre composites has been done in the USA[21-23]. However, indications are that bolted joints for composites can be structurally efficient and more important that they can also be cost-effective. For these reasons a programme of research was initiated in Structures Department, RAE, to evaluate bolted joints in CFRP and to compare them with other jointing techniques.

This Report describes tests to determine the basic properties of multi-directional CFRP around a central circular hole in a plate loaded in tension by means of a pin in the hole (single-hole joint). Multi-hole tests are also described which provide an extension to the data obtained from the single-hole tests and allow the measurement of any interaction effects between holes in various bolt groups. Results are presented for several types of multi-directional CFRP laminate and are discussed in terms of possible optimum bolted joint design.

2 POTENTIAL FAILURE MODES IN CONVENTIONAL MATERIALS

Apart from failure of the bolt in either shear or compression, bolted joints in isotropic materials fail in one of three potential modes, namely tension, bearing or shear. Tensile failure normally occurs at the minimum cross-section, probably across a line of bolts where the stress concentration is a maximum. Failure initiates at a hole edge and propagates in a direction normal to that of the applied load, i.e. across the width of the joint. The joint strength is usually quoted in terms of a net ultimate tensile strength and is given by

$$\sigma_{net(ult)} = \frac{L_{(ult)}}{(W - nd)t} , \qquad (1)$$

where $L_{(ult)}$ is the tensile failing load, W the joint width at the net section, n the number of holes of diameter d occurring at that section and t the joint thickness.

Bearing failure is the result of a local compressive failure in material immediately beneath the loaded bolt. As both bolt and hole are usually circular in cross-section the magnitude of the compressive stress varies around the circumference. However, it is usual practice when deriving bearing stress to assume the applied load, $L_{(ult)}$, acts uniformly on the cross-section, in which case the ultimate bearing stress is given as

$$\sigma_{b(ult)} = \frac{L_{(ult)}}{ndt} . \qquad (2)$$

As compressive failure in isotropic materials is generally difficult to define, ultimate bearing strengths are normally taken to be the 2% tensile proof stress.

Failure of the joint in shear, usually called shear pull-out, is a result of shear failure in the two parallel planes which are tangential to the

hole edge and extend to the free edge in a direction parallel to the applied load.

The ultimate shear strength of a bolted joint is therefore given by

$$\tau_{xy(ult)} = \frac{L_{(ult)}}{2et} \quad , \tag{3}$$

where $L_{(ult)}$ is the failing shear load and e is the distance between hole centre and free edge parallel to the applied load and usually known as the edge distance.

3 POTENTIAL FAILURE MODES IN COMPOSITE MATERIALS

3.1 Factors affecting failure

High performance fibre reinforced plastic components can be considerably weakened by the introduction of holes and cut-outs, due partly to the large stress concentrations[24] that occur in the region around such discontinuities and partly to a lack of plasticity. For example, by virtue of the high degree of anisotropy of unidirectional carbon fibre reinforced plastics (CFRP), the tensile elastic stress concentration factor due to a circular hole in a large sheet can be as large as 8 in contrast to the much lower value of 3 normally associated with isotropic materials[25]. Furthermore, as most isotropic materials exhibit some plasticity, yielding can take place in highly stressed regions and the effect of stress concentrations on the final net failing stress is small; such is not the case for unidirectional CFRP which is generally elastic to failure[26] and the effect of stress concentration is to give rise to correspondingly low net failing stress. It comes as no surprise, therefore, that the efficiency of bolted joints in unidirectional CFRP is very low indeed.

However, if in the region of the bolt holes the degree of anisotropy could be reduced and some plastic or pseudo-plastic behaviour introduced then efficiency might be expected to increase considerably. Fortunately, such joint 'softening' can be readily achieved by the incorporation of fibre oriented in different directions and, moreover, with the use of preimpregnated unidirectional sheet material to form multi-directional multi-ply laminates, this can be done without a significant increase in fabrication complexity. (It is worth noting here that joint softening might also be achieved by other techniques such as by the incorporation of other types of fibrous material, for example glass fibre or Kevlar. However, this is not under consideration at present but may be the subject of a further investigation.)

Before efficient bolted joints can be produced using multi-directional laminates, two important questions must be answered; which fibre orientation give the most effective properties and what proportion of these oriented plies are necessary to achieve them? It follows that each of the three potential joint failure modes requires examination for each of these variables so that favourable laminate combinations can be produced. Other variables which also need to be considered are ply stacking sequence, fibre type, specimen geometry, degree of clamping of the loading pin, loading pin diameter and laminate thickness.

3.2 Tension

As with conventional materials, the tensile load required to fail an otherwise uniform, plain laminate, through a cross-section at which holes occur (net section) is less than at the section at which there are no geometric inclusions (gross section). The stresses at these sections, at failure, are given by

$$\sigma_{net(ult)} = \frac{L_{(ult)}}{(W - nd)t} \tag{4}$$

and

$$\sigma_{gross(ult)} = \frac{L_{(ult)}}{Wt} , \tag{5}$$

where $L_{(ult)}$ is the failing load of the member. The tensile strength efficiency achieved at these sections can be expressed in the form of average net and gross stress concentrations given by

$$k_{net} = \frac{\sigma_{x(ult)}}{\sigma_{net}(ult)} \tag{6}$$

and

$$k_{gross} = \frac{\sigma_{x(ult)}}{\sigma_{gross(ult)}} , \tag{7}$$

where $\sigma_{x(ult)}$ is the theoretical ultimate tensile strength of the plain laminate.

The theoretical ultimate tensile strength of a multi-directional laminate containing plies at 0^{o} and $\pm\alpha^{o}$ to the direction of the applied load can be

calculated with adequate accuracy using a law of strain compatability provided the elastic range of the material is not exceeded. Let the load carried by the 0° plies be P_0 and the total load carried by all plies be P ; then

$$P = \left(\frac{t_0E_0 + t_\alpha E_\alpha}{t_0E_0}\right)P_0 \tag{8}$$

where t_0 and t_α are the total thicknesses of the 0° and $\pm\alpha^{\circ}$ plies in the laminate respectively and E_0 and E_α are the corresponding Young's moduli. Given that $\sigma_{f(ult)}$ is the tensile strength of the fibre and v_f the volume fraction of fibres in the laminate it follows that

$$P_{0(ult)} = \sigma_{f(ult)}v_fA_0 \quad , \tag{9}$$

where A_0 is the cross-sectional area of the 0° plies.

On the normally valid assumption that the 0° fibres will fail at a lower strain than the $\pm\alpha^{\circ}$ fibres, it also follows that

$$P_{(ult)} = \left(\frac{t_0E_0 + t_\alpha E_\alpha}{t_0E_0}\right)\sigma_{f(ult)}v_fA_0 \quad .$$

Finally, the tensile failing stress, $\sigma_{x(ult)}$, of the complete laminate is given by

$$\sigma_{x(ult)} = \left(\frac{t_0E_0 + t_\alpha E_\alpha}{t_0E_0}\right)\sigma_{f(ult)}v_f\frac{A_0}{A} \quad , \tag{10}$$

where A is the cross-sectional area of the complete laminate. However this equation does not hold true for $\pm45^{\circ}$ laminates where failure under tensile loading occurs by in-plane shear on the 45° plane to the axis of loading. In this case the tensile failing stress is given by

$$\sigma_{x(ult)} = 2\tau_{xy(ult)} \tag{11}$$

where $\tau_{xy(ult)}$ is the in-plane shear strength of the material.

3.3 Bearing

The bearing strength of a composite material, like that of a conventional material (equation (2)), is usually expressed as an average stress in the form

$$\sigma_{b(ult)} = \frac{L_{(ult)}}{ndt} .$$

It is known from early compression tests[27] carried out on unidirectional CFRP that a substantial degree of lateral constraint at the ends of a compressive specimen is necessary to prevent premature end failure due to a breakdown in the fibre resin interface and a consequent brush-like failure. Bearing of a pin in a hole gives rise to similar compressive stresses in the material around the hole and it is therefore to be expected that lateral constraint will influence the magnitude of the composite ultimate bearing strength. Hence the degree of lateral constraint is likely to be an important parameter in the determination of bearing strength.

3.4 Shear

The shear strength normally quoted for a composite is the interlaminar shear strength. Unfortunately, except for some unidirectional materials in which isotropy can be assumed on all planes normal to the fibre direction, it is of little use in the estimation of joint shear strengths where failure is due to in-plane shear stresses. In-plane shear strength can be measured using the rail shear test but, due to shear stress concentrations around a loaded hole, it is unlikely to be a representative test. Shear strengths are therefore measured using pin shear pull-out. The strength in this case, as for conventional materials (equation (3)), is given as

$$\tau_{xy(ult)} = \frac{L_{(ult)}}{2et}$$

4 SINGLE-HOLE EXPERIMENTS

4.1 Material selection and laminate manufacture

Four types of multi-directional laminate were chosen as representative of those likely to be used in airframes; $0^\circ \pm 45^\circ$, used in compression structures, $\pm 45^\circ$, used in shear structures, $0^\circ/90^\circ$, used in bi-directional stress situations and $0^\circ \pm 60^\circ$, used because of its pseudo-isotropic properties.

All laminates were made from high strength carbon fibre type 130SC/10000 (also known as Type 2 or HTS) released to MOD Provisional Specification NM565[28], preimpregnated with an epoxy resin system (Union Carbide ERLA 4617/DDM*) to

---

* Diaminodiphenylmethane.

MOD Provisional Specification NM547[29] to form unidirectional warp sheets of nominal thickness 0.25mm.

Standard laminates were made from 12 plies, (see Fig.1 for orientations and stacking sequences), and balanced about the mid-plane both to prevent thermal distortion during manufacture and to eliminate bending and twisting when under tension. The laminates were press-moulded using a combination of matched metal moulding and bleed-cloth techniques (see for example Collings and Ewins[30]) giving finished laminates of thickness 3mm and fibre volume fraction 0.6. The woven appearance of the finished laminates, clearly visible in Figs.11, 15, 21, 27 and 34, is caused entirely by the pattern left by the bleed cloth; all laminates were made using combinations of unidirectional warp sheet only. Laminates of 18 ply and 24 ply, of thicknesses 4½mm and 6mm respectively, were made using the same manufacturing process; the stacking sequences used are given in Fig.2. These thicker laminates were needed for an investigation into the effect of laminate thickness on bearing strength.

4.2 Testing variables

Three different hole diameters were chosen from a range most likely to be used in bolted airframe assemblies; these were 6.35mm (¼in) 9.53mm (⅜in) 12.7mm (½in).

For each type of laminate and for each hole diameter the values of edge distance, e, and specimen width, W, were varied to produce each of the three primary modes of failure. The values of e and W were also chosen so that failure in one mode was relatively unaffected by a tendency to fail in either of the other two. This was achieved from preliminary experiments, the results of which are given in Figs.3 to 6. Figs.3 and 4 show the change of failure mode from one of tension to one of bearing as the ratio W/d is increased while Figs.5 and 6 show the change of failure mode from one of shear to one of bearing as the ratio e/d is increased. Preparation and testing of specimens for the preliminary experiments were carried out in a similar manner to that described in section 4.3 below.

An investigation of the effect of lateral constraint on bearing strength required a knowledge of the relationship between bolt torque and lateral constraint, bolt torque being considered the most suitable method by which lateral constraint could be applied. For this relationship reference was made to Stewart[31] who has shown that, for unlubricated steel bolts loaded in tension by means of an applied torque, the tensile load in the bolt, P_t, is given by

$$P_t = \frac{T}{Kd} \quad , \tag{12}$$

where T is the applied torque and K is a torque coefficient. This coefficient was measured by Stewart and found to be substantially constant at a value of 0.2 for all bolt diameters and for both coarse and fine threads. Since lateral constraint is also area dependent, the clamped area around the loading pin was constrained to be equivalent to that of a standard washer, the diameter, D, of which is expressed as a function of hole diameter, d, as

$$D = 2.2d \quad . \tag{13}$$

It follows that, as the chosen constraint area is a function of hole diameter, lateral constraint can be expressed as a transverse compressive stress, σ_z, where

$$\sigma_z = \frac{P_t}{\pi/4(D^2 - d^2)} \quad . \tag{14}$$

Substituting for D, K and P_t gives a simplified expression for the constraint stress as

$$\sigma_z = 1.658 \frac{T}{d^3} \quad . \tag{15}$$

For a $0^\circ \pm 45^\circ$ laminate using the stacking sequence shown in Figs.1 and 2 and for all hole diameters, the laminate thickness and lateral constraint were varied to determine the effect each would have on ultimate bearing strength. The laminate thicknesses chosen were 12 ply (3mm), 18 ply (4½mm) and 24 ply (6mm).

4.3 Specimen preparation and testing

The test specimen, shown diagrammatically in Fig.7, consisted of a rectangular strip of laminate of constant thickness t, width W and length approximately 200mm, with the 0° ply fibre axis parallel to the length. Each end of the specimen was prepared with a circular hole centrally placed with respect to the width and at a predetermined distance from the end.

Test specimens were cut from a laminate using a small band saw and, to reduce the effect of edge defects on specimen failure, all cut edges were

finished with a fine abrasive. The holes were prepared using a vertical bench drill by first drilling a pilot hole of 3mm diameter through the laminate and then opening up the hole with a rotorborer. To prevent damage to the outer plies of the laminate, the holes were bored partly through from each side the pilot hole ensuring accurate location of the rotorborer. Each hole was finished using a standard reamer of a tolerance conforming to British Standard BS164[32]; this tolerance is sufficient to allow a 'precision run' fit (H7-f7 to British Standard BS1916[33]) to be obtained between loading pin and hole.

Test specimens were loaded in tension using a 100kN Avery test machine. Load was applied to the specimen by means of shear (or loading) pins and loading lugs made from S96 steel. The loading assembly is shown in Fig.8. Specimens were loaded at a constant rate ensuring failure in about 30s. The mode of failure and maximum load were recorded for each specimen, and the mean failing load for similar specimens calculated from a sample of two to four specimens. To allow for the effect on failing loads of small fluctuations in moulded thicknesses, all results were normalised to the effective thickness at a fibre content of 60% by volume.

To control the clamping area around the loaded hole, small raised pads equivalent in area to a standard washer were machined onto the loading lugs; these were used in preference to washers in order to reduce pin bending. A further reduction of pin bending was obtained by tolerancing both loading pin and holes in the loading lugs to a precision fit. The required lateral constraint was applied by means of a known torque (see section 4.2). For tests requiring no lateral constraint it was necessary to ensure that the loading lugs were clear of the specimen faces to allow for the lateral expansion of the laminate around the hole when under load. However, clearance was again minimised in order to reduce pin bending.

4.4 Results

Ultimate net tensile strengths for $0^\circ \pm 45^\circ$ and $\pm 45^\circ$ laminates are given in Fig.9 and for $0^\circ/90^\circ$ and $0^\circ \pm 60^\circ$ laminates in Fig.10. Photographs of typical failures in each of the four laminate types are shown in Fig.11. The fibre tensile strength required for the calculation of $\sigma_{x(ult)}$ (equation (10)) was determined from a 0° laminate using a standard test specimen and test technique[34] and found to be $2.9GN/m^2$. The values of the corresponding Young's moduli, also required for the calculation of $\sigma_{x(ult)}$, were $E_0 = 130GN/m^2$ and $E_{45} = 17GN/m^2$. Using equation (10), the value of $\sigma_{x(ult)}$ for a plain

$\frac{1}{3}$ 0°, $\frac{2}{3}$ $\pm 45^{\circ}$ laminate was calculated to be 730MN/m^2. Calculation of the tensile strength of a plain $\pm 45^{\circ}$ laminate was made, using equation (11) and the measured interlaminar shear strength[35] of a 0° laminate (82MN/m^2), and found to be 164MN/m^2. The interlaminar shear strength was used in this calculation because it has been shown to be of the same magnitude as the in-plane shear strength of a $\pm 45^{\circ}$ laminate (see for example Snell[36]). Stress concentration factors of two laminate types, $0^{\circ} \pm 45^{\circ}$ and $\pm 45^{\circ}$, are given in Figs.12 and 13.

Bearing strengths for the four laminate types with a 6.35mm diameter hole and a lateral constraint of 22MN/m^2 are given in Fig.14. Photographs of typical bearing failures in each of the laminate types are shown in Fig.15. The variation of bearing strength with lateral constraint for different hole diameters for a $0^{\circ} \pm 45^{\circ}$ laminate is given in Fig.16. Bearing strength as a function of lateral constraint for $0^{\circ} \pm 45^{\circ}$ laminates of different thicknesses and different hole diameters are given in Figs.17 to 19. The effect of d/t ratio on bearing strength, without lateral constraint at the loaded hole, is given in Fig.20. A photograph of an unconstrained bearing failure is shown in Fig.21.

The joint shear strengths of the four laminate types as a function of edge distance are presented in Fig.22. Photographs of typical failures in each of the laminates are shown in Fig.23.

5 MULTI-HOLE EXPERIMENTS

5.1 General remarks

The results obtained from single hole tests allow optimisation for minimum joint weight using a single bolted connection. However multi-hole joints, used to increase the load carrying efficiency of a structure and of more interest in aircraft design where sheet material is to be joined, still need to be evaluated. The evaluation of these joints was carried out using three hole groupings as shown in Fig.24. Of these groups, the two-hole 'in tandem' was used to increase the data already gained from single-hole experiments on the effect of specimen width on ultimate tensile strength and to determine, if any, the interaction between holes due to shear and/or bearing stresses. A four-hole group consisting of two 'tandem' joints side-by-side was used to produce tensile failure in wide specimens. This enabled the tensile interaction to be determined by comparing the ultimate tensile failing strength of single 'in tandem' specimens of width W with double 'in tandem' specimens of width $2W$. The third hole

group, two holes side-by-side, was used for specimen widths that were too wide to fail in tension using a single hole. This enabled the tensile interaction of holes to be determined in a similar way to the single and double 'tandem joints'.

5.2 Test variables

Tensile tests were carried out on the three hole groups using a $0^{\circ} \pm 45^{\circ}$ laminate with a stacking sequence as shown in Fig.1b. This laminate configuration was chosen because it was found to be the most efficient of those tested in the single-hole tests. Spacing of holes for all joint groups was chosen from single-hole test data on the assumption that no interaction exists. To enable the full bearing strength to be achieved without shear-out failure occurring, the distance between hole centres along the load axis line was taken as $e + d/2$, thereby ensuring the same edge distance as for the single-hole tests. The side-by-side spacing between centres was chosen as W (see Fig.25), where W is the specimen width per bolt hole across one section, and $W/2$ the side distance. A basic hole diameter of 6.35mm was chosen since this size had been shown to be most efficient in the single-hole tests. The bolts were tightened to a torque of 3.4N m which ensured sufficient lateral constraint around the hole to achieve the full bearing strength. Using the data of Fig.5, the required value of $e + d/2$ was calculated to be not less than 23.75mm and therefore both edge and centre distances were chosen to be 25mm.

5.3 Specimen preparation and testing

Specimens were prepared as for the single-hole experiments but with the additional use of a drilling jig to ensure alignment between the hole groups at each end of the specimen. This alignment ensured that no in-plane rotation of the joint could occur, so preventing turning moments from altering both the distribution and vectoring of loads on each of the loading pins.

The specimens were tested as for the single-hole specimens except that load was transmitted to the specimen by means of flat aluminium alloy tension plates. High tensile steel bolts were used as loading pins. To prevent uneven loading of the bolts in double-row bolt groups, the in-plane stiffness of the tension plates was matched to that of the specimen being tested.

5.4 Results

The net tensile strength of multi-hole tests, using a 6.35mm diameter loaded hole, plotted as a function of W, the specimen width per bolt hole, are shown in Fig.25. Tensile results for both single and multi-hole experiments

are given in Fig.26 and are expressed in the form of average stress concentrations k_{net} and k_{gross}. Photographs of failed specimens from each of the hole groups are given in Fig.27.

Using the results given in Fig.26, two joint configurations were compared (see Fig.28) to demonstrate the efficiency of both multi-hole and single-hole joints. Let efficiency in terms of joint weight per unit load carried ($\varepsilon_{(d)}$) be defined as

$$\varepsilon_{(d)} = \frac{W_{(d)}}{L_{(ult)}} , \qquad (16)$$

where $W_{(d)}$ is the joint weight (not including bolts) taken over a length ℓ and arbitrary width W (see Fig.28). Then, from Fig.26 and equations (7) and (5), a joint consisting of a single 12.7mm diameter bolt gives $L_{(ult)} = 26.87$kN and $W_{(12.7)} = 27.7$g. Substitution into equation (16) gives $\varepsilon_{(12.7)} = 1.031$g per kN load carried. Similarly a joint consisting of two 6.35mm diameter bolts in 'tandem' gives $L_{(ult)} = 32.49$kN and $W_{(6.35)} = 34.06$g, so that $\varepsilon_{(6.35)} = 1.048$g per kN load carried. If bolt weights were taken into consideration the latter joint would show a marked advantage, but this has not been done since it is unlikely that a 12.7mm diameter bolt would be anything approaching optimum for connecting sheets of 3mm thickness and a false impression of weight saving might therefore be given.

6 OTHER VARIABLES INFLUENCING JOINT PROPERTIES

6.1 Ratio of 0° to $\pm\alpha^\circ$ fibres in a $0^\circ \pm \alpha^\circ$ lay up

To determine the optimum ratio of 0° to $\pm\alpha^\circ$ fibres, single-hole tests were conducted on several laminates using the same overall method described previously and stacking sequences shown in Figs.1b, 1d, 29a and 29b. The five lay-ups employed and proportions of 0° to $\pm 45^\circ$ plies were (i) unidirectional, (ii) $\frac{1}{3}$ 0°, $\frac{2}{3}$ $\pm 45^\circ$, (iii) $\frac{1}{2}$ 0°, $\frac{1}{2}$ $\pm 45^\circ$, (iv) $\frac{2}{3}$ 0°, $\frac{1}{3}$ $\pm 45^\circ$ and (v) $\pm 45^\circ$. Tension, bearing and shear properties were measured using a 6.35mm diameter hole and test procedure as described in section 4.3. In the case of the unidirectional material bearing tests were carried out using the rig shown in Fig.30, one specimen being transversely restrained to prevent premature splitting of the specimen and another specimen being left unrestrained and allowed to fail through longitudinal splitting. Tension tests were not carried out on unidirectional material due to the high ratio of tensile to shear strength; the specimen width would be so impractically small as to make any test result of doubtful value.

The results of the tests are plotted in Figs.31 to 33, Fig.33 showing all three properties measured as a function of proportion of $\pm 45^{\circ}$ fibres. A photograph of a failed unidirectional specimen which has been restrained transversely to produce a bearing failure is given in Fig.34.

6.2 Stacking sequence

The plies in a laminate can be stacked in more than one sequence throughout the thickness and it is possible that this could affect some laminate properties significantly. In order to try and assess this affect, two $0^{\circ} \pm 45^{\circ}$ laminates, each using a $\frac{2}{3}$ 0°, $\frac{1}{3}$ $\pm 45^{\circ}$ lay up, were manufactured and prepared as described in sections 4.1 and 4.3. Two different stacking sequences were used and are shown in Figs.29b and 35. The laminates were tested as described in section 4.3 using a 6.35mm diameter hole.

Results of the tests showed that there was only a 2% difference between shear strengths and a 6% difference between tensile strengths for the two laminates. Bearing strength however, was significantly different, giving a drop in bearing strength of 16% for the less homogeneous lay up (Fig.35) compared with the bearing strength of the more homogeneous lay up (Fig.29b). The values of bearing strengths were respectively $778 MN/m^2$ and $929 MN/m^2$.

7 DISCUSSION AND CONCLUSIONS

7.1 Tensile behaviour of single-hole joints

The results of the single-hole tests show a number of significant features and enable a clear picture to emerge of the likely performance of CFRP bolted joints. Looking at the tensile performance, it is evident from the data presented in Figs.9 and 10 that the ultimate tensile strength of a single-hole joint is strongly dependent on ply orientation, hole size and specimen width. It is also clear that the best overall performance is exhibited by $0^{\circ} \pm 45^{\circ}$ laminates and some reasons for this are worth considering in more detail.

When presented in the form of tensile stress concentrations, it is seen that the average net stress concentration for a simple $\pm 45^{\circ}$ laminate (Fig.13) is about 1.2 and is almost independent of both hole size and specimen width. In contrast it is known[24] that for a unidirectional (0°) laminate with a circular unloaded hole, loaded in tension at its ends, the maximum tensile stress concentration can be as large as 7 or 8. This suggests that in single-hole joint form the presence of $\pm 45^{\circ}$ plies in a $0^{\circ} \pm 45^{\circ}$ laminate could reduce the value of the net stress concentration by imparting a degree of 'softening' to the joint. Experimental evidence for this is to be found in tests carried

out on $0^{o} \pm 45^{o}$ laminates in which the ratio of 0^{o} plies to $\pm 45^{o}$ plies was varied (see section 6) and the results plotted in terms of average net and gross tensile stress concentrations (Fig.36). There is a monotonic relationship between the value of the stress concentration and the proportion of $\pm 45^{o}$ plies, varying from a gross value of 1.5 for an all $\pm 45^{o}$ laminate to about 6 when extrapolated to the unidirectional (all 0^{o} plies) case. The magnitude of the stress concentration at the hole edge has been derived theoretically by Lekhnitski[38] and, for a plate pierced by a hole and loaded in tension at the ends, it is given as

$$k_{gross} = 1 + \sqrt{2\left(\sqrt{\frac{E_1}{E_2}} - \nu_{12}\right) + \frac{E_1}{G}} \qquad (17)$$

where E_1 is Young's modulus in the direction of the load axis,
E_2 is Young's modulus in the direction normal to the load axis,
G is the in-plane shear modulus and
ν_{12} is the principal Poisson's ratio.

Substitution of the relevant properties for each laminate type yields the gross stress concentrations which are shown in Fig.36 plotted as a function of the proportion of $\pm 45^{o}$ plies. Although the formula is strictly for an unloaded hole, the variation in stress concentration with the proportion of $\pm 45^{o}$ plies is of identical form to that derived experimentally for the single-hole loaded joint. Furthermore, since for any particular proportion of $\pm 45^{o}$ plies the values of the stress concentration for the unloaded hole and single-hole joint are similar, it can be concluded that the effect on the stress concentration of loading the hole is small.

The extrapolated data using the Lekhnitski formula has also been used to derive expected tensile performance of unidirectional (0^{o}) laminate joints and the data is included in Fig.33. Using all the data, both experimental and derived, it can be seen that the best tensile performance is achieved using about 30% to 50% of $\pm 45^{o}$ plies in a $0^{o} \pm 45^{o}$ laminate. This will be reviewed later in the discussion in terms of the bearing and shear performance. However, it is worth noting here that the failing stress is relatively constant over a wide range of proportions of 0^{o} to $\pm 45^{o}$ plies and this indicates that the tensile stress concentrations vary proportionally with the mean tensile strength of the plain laminate. Such a result may have implications in joint design since it appears that a range of stress concentrations can be obtained with

little change in the load carry capacity of the joint; a similar result might be expected for the general case of cut-outs in $0^{\circ} \pm 45^{\circ}$ laminates with similar implications.

The results for the remaining two types of laminate studied, $0^{\circ} \pm 60^{\circ}$ and $0^{\circ}/90^{\circ}$, show that a degree of joint 'softening' is obtained by the use of $\pm 60^{\circ}$ or 90° plies but that the effects are less pronounced. This is to be expected since $\pm 45^{\circ}$ plies exhibit a unique combination of elastic properties, together with high failure strains, not shared to the same extent by other ply orientations.

The effect of a change in specimen geometry, or more particularly a change in the ratio of hole diameter to specimen width, is clearly shown in Figs.9 and 10; the effect is most marked for $0^{\circ}/90^{\circ}$ laminates and least for $\pm 45^{\circ}$ laminates. Such sensitivity to specimen width has also been demonstrated by Waddoups, *et al.*[37] in tests carried out on pierced laminates loaded in tension at the ends where the value of the gross stress concentration was found to increase with hole diameter. Other work by Kulkarni, Rosen and Zweben[39] has shown that a shear lag analysis, which takes due account of material heterogeniety, adequately explains the hole size-effect in laminates loaded in tension at the ends and indeed predicts results which are in substantial agreement with those of the present study.

A comparison of the specific tensile strength of bolted joints in CFRP with those in isotropic metals is made in Table 1 where it can be seen that, although CFRP suffers a larger loss of efficiency due to the presence of larger stress concentrations, there is a distinct advantage to be gained over conventional materials. Expressed in terms of the ratio of specific strengths of CFRP and metals the potential advantage varies from 1.32 to 1.52 when compared with L71 aluminium alloy and from 1.79 to 2.07 when compared with S96 steel. The comparison is made on the basis that, as metals generally exhibit considerable yielding, the stress concentrations in the metals at failure are negligible. However, such a situation is rather artificial since metal joints are normally designed to work within the elastic region and an arguably better comparison should take account of the stress concentrations in metal joints. On such a basis CFRP joints would compare even more favourably. Nonetheless, it should be borne in mind that, for CFRP, secondary stresses such as shear and transverse in-plane tension may significantly affect the fatigue life and adversely affect the performance of CFRP joints in comparison with metal joints.

Furthermore the design of CFRP joints would probably need to take account of reduced design allowables, based on an analogous concept to that of proof stress in metals; if overall airworthiness requirements are to be met. The whole subject of design allowables, together with those of fatigue and other environmental effects would need to be studied before the overall potential advantage of CFRP could properly be ascertained.

7.2 Bearing behaviour of single-hole joints

The bearing strength of single-hole bolted joints in CFRP has been shown to be dependent on five main variables; degree of lateral constraint around the hole, ply orientation, ratio of 0° plies to $\pm\alpha^\circ$ plies, ply stacking sequence and laminate thickness. Looking first at the results of variation of bearing strength with lateral constraint pressure (applied normal to the plane of the laminate) for $0^\circ \pm 45^\circ$ laminates, shown in Fig.16, it can be seen that improvements from 60 per cent to 170 per cent according to hole size can be achieved with constraint pressures of up to $22MN/m^2$; at higher constraint pressures little further improvement is realised. It is significant that differences in bearing strength for various hole sizes which are so marked in the unconstrained condition virtually disappear at constraint pressures of $22MN/m^2$. These results lend yet further weight to the now well-known arguments[27] that lack of fibre support at a compressive interface, in this case the loaded half of the hole, can lead to premature compressive failure. A clear example is given in the photograph of Fig.21 which is of a failed unconstrained specimen; the local buckling or brush-like failure is clearly evident.

Examination of the failed regions of constrained specimens of all four laminate types indicates that failure has occurred by the initiation of shear cracks (through both fibres and matrix) at the hole edge and subsequent propagation to the edge of the clamped region where the mode has tended to revert to one of local instability and delamination (*cf.* unconstrained specimens). The photographs of failed constrained specimens, shown in Fig.15, show clearly the mode change from the constrained to unconstrained regions. A further study of the failed specimens reveals that the fibre orientations have a definite influence on the position around the hole circumference (θ) at which failure is initiated. For the single $\pm45^\circ$ and $0^\circ \pm 45^\circ$ laminates failure has initiated at a point on the circumference at 45° to the loading axis (i.e. $\theta = 45^\circ$). For the $0^\circ/90^\circ$ laminates failure has initiated on the load axis (i.e. $\theta = 0^\circ$) and for $0^\circ \pm 60^\circ$ laminates failure initiation is at approximately 30° to the load axis (i.e. $\theta = 30^\circ$). These results are in general agreement with the theory

proposed by Waszczak and Cruse[43] in which it is suggested that failure initiation occurs at points on the circular boundary where fibres are either tangential or normal to the boundary.

The effect of ply orientation on bearing strength for the constrained case is shown clearly in Fig.14 and among the four laminate types is perhaps not as pronounced as might have been expected. There is little difference between the bearing strengths of $0^\circ \pm 45^\circ$ and $0^\circ \pm 60^\circ$ laminates (with plies in the ratio $\frac{1}{3}$ at 0° to $\frac{2}{3}$ at $\pm 45^\circ$), each achieving a mean value of about $900 MN/m^2$. There is a significant if small reduction in the bearing strength realised in $\pm 45^\circ$ laminates (mean strength of about $830 MN/m^2$) and a further reduction for $0^\circ/90^\circ$ laminates (mean value of $800 MN/m^2$).

As might be expected, the bearing strength is dependent on the ratio of 0° plies to $\pm\alpha^\circ$ plies in a $0^\circ \pm \alpha^\circ$ laminate and the effect is best demonstrated by reference to the results obtained for $0^\circ \pm 45^\circ$ laminates (see Fig.33). As 0° plies are introduced into a $\pm 45^\circ$ laminate so the constrained bearing strength increases from about $830 MN/m^2$ up to a maximum of $930 MN/m^2$ for laminates in which the 0° plies account for some 60 per cent of the total. The mode of failure in all cases is essentially that of compression in the fibre direction in each of the individual plies giving rise to an overall compressive failure. Further increases in the percentage of 0° plies, however, leads not only to a reduction in bearing strength but also to a change of failure mode. In the absence of adequate in-plane transverse restraint, failure occurs by longitudinal splitting (i.e. in the direction of the loading axis) at equivalent bearing stress levels which for a unidirectional laminate (i.e. all 0° plies) are as low as $500 MN/m^2$. The reasons for a mode change and associated low failing stress are not hard to find since the in-plane transverse stresses due to a loaded hole can be significant, particularly in comparison with the relatively low transverse strength of unidirectional material, and are probably large enough to cause transverse failure. Indeed, subsequent strain gauging of a single-hole unidirectional specimen revealed maximum transverse strains around the hole at failure of 700 microstrain which is in good agreement with the ultimate strains recorded by Mead[40] during transverse tensile tests on similar material.

Tests were also carried out on unidirectional specimens which were transversely restrained in-plane to prevent the longitudinal splitting mode of failure and these resulted both in an increase in bearing failing stresses up to a mean value of about $860 MN/m^2$ and in a mode change to one closely similar to true compressive failure (see the photograph of Fig.34). Since both the mode

of failure and the failing stress are similar to those observed in $0^{\circ} \pm 45^{\circ}$ laminates, it can reasonably be concluded that at least part of the function of $\pm 45^{\circ}$ plies in a $0^{\circ} \pm 45^{\circ}$ laminate is to offer adequate in-plane transverse restraint against longitudinal splitting.

If it can be assumed that a transversely restrained unidirectional joint specimen fails in a truly compressive mode then the ratio of the ultimate longitudinal compressive strength of the material to the bearing stress of the joint at failure (in this case $860 MN/m^2$) is a measure of the compressive stress concentration due to the loaded hole. The longitudinal compressive strength of the material was measured using a standard test specimen and test technique[30] and found to be $1370 MN/m^2$, so on this basis the stress concentration is 1.59 (= 1370/860). Since it is known that the introduction of $\pm 45^{\circ}$ plies reduces the mean compressive strength of the material while at the same time increasing the bearing strength, it follows that the stress concentration is alleviated by the inclusion of $\pm 45^{\circ}$ plies. For isotropic materials, assuming a cosine distribution of stress over the loaded half-hole circumference, the stress concentration is given by Bickley[41] as 1.274 although it has been shown by Frocht and Hill[42] that the fit between the loading pin and hole can significantly alter both the magnitude and the position of the maximum stress concentration. Nonetheless, the evidence is that $0^{\circ} \pm 45^{\circ}$ laminates exhibit bearing stress concentrations and efficiencies similar to those existing in isotropic metals.

The distribution of plies throughout the laminate thickness, usually referred to as the ply stacking sequence, has been shown to have a significant influence on the magnitude of the ultimate bearing strength. Results of tests on $0^{\circ} \pm 45^{\circ}$ laminates ($\frac{2}{3}$ at 0° and $\frac{1}{3}$ at $\pm 45^{\circ}$) of various but balanced stacking sequences (see Figs.29b and 35) show that the less homogeneous sequences exhibit significantly lower bearing strengths. A value of $778 MN/m^2$ was recorded for the less homogeneous stacking sequence as compared with a value of $930 MN/m^2$ for the more homogeneous, a strength reduction of about 16 per cent. Although further work would be required before the reasons for the differences are fully understood, it is probable that the higher interlaminar shear stresses that exist in the less homogeneous stacking sequences are a major cause of the reduction. However, the implications are clear and in general the most homogeneous stacking sequences should be used in order to maximise bearing strengths.

The effect of laminate thickness on bearing strength for $0^{\circ} \pm 45^{\circ}$ laminates ($\frac{1}{3}$ at 0° and $\frac{2}{3}$ at $\pm 45^{\circ}$) and various hole diameters is shown in

Figs.17 to 19 and it is clear that, provided adequate lateral constraint is applied, little thickness effect exists. If lateral constraint is not applied then large variations in bearing strength can exist and when plotted against the ratio of hole diameter (d) to laminate thickness (t), as in Fig.20, it can be seen that there is a monotonic fall-off in strength as the ratio d/t increases. Such a result is similar to that observed in other materials, including metals, where the efficiency of joints has been found to depend on the d/t ratio. It is of interest to note that the results were derived using three hole sizes and three laminate thicknesses and the smooth curve of bearing strength against d/t ratio is an indication of good consistency of test results.

A comparison of specific bearing strengths of CFRP laminates with some isotropic materials is made in Table 2 and the potential advantage offered by CFRP over both aluminium alloys and steels is clearly indicated.

7.3 Shear behaviour of single-hole joints

As might be expected from a knowledge of the in-plane shear strength of multi-directional CFRP laminates, the shear pull-out strength of single-hole joints has been shown to be strongly dependent on the ply orientations within the laminate. The shear pull-out stress at failure of a unidirectional laminate, loaded in the fibre direction, is as low as $23MN/m^2$, whereas the in-plane shear strength of a plain unidirectional laminate made from similar material is about $85MN/m^2$. Although the stress distribution around the loaded hole is complex with significant transverse in-plane stresses, the difference between the two tends to indicate the presence of significant shear stress concentrations around the loaded hole. In contrast, the shear pull-out stress at failure of a pseudo-isotropic ($0^\circ \pm 60^\circ$) laminate is approximately $150MN/m^2$ (Fig.22) and since it is relatively insensitive to edge distance it can be concluded that the shear stress concentration is relatively small. These effects are analogous to those of bearing where a reduction in the degree of anisotropy together with a strengthening of potentially weak planes of failure leads both to an increase in strength and a decrease in the magnitude of the stress concentration.

The shear pull-out failing stress of $0^\circ/90^\circ$ laminates varies little with edge distance and again it can reasonably be concluded that the stress concentrations are small. Further evidence for this is to be found in the comparison of the measured pull-out strengths of $0^\circ/90^\circ$ laminates of about 70 to $80MN/m^2$ with the known in-plane shear strength of similar unidirectional laminates of about $85MN/m^2$. Since $0^\circ/90^\circ$ laminates constitute a special case

of multi-directional laminates in that both the in-plane shear stress/strain behaviour and the in-plane shear strength are theoretically the same as those of similar unidirectional material, the ratio of the two values is a measure of the shear stress concentration and this is clearly small.

The results of shear pull-out tests carried out on $0^{\circ} \pm \alpha^{\circ}$ laminates ($\alpha = 45^{\circ}$ or 60°) for varying proportions of $\pm\alpha^{\circ}$ plies show that the highest strengths are achieved using about 50 per cent of $\pm\alpha^{\circ}$ plies (see Figs.31 and 33). Such a result is favourable in terms of joint design since it corresponds well with optimum ratios for maximum bearing and tensile strengths and is not inconsistent with combinations of plies likely to be used in many design situations.

Comparison of specific shear strengths with other materials is made in Table 3 where it can be seen that CFRP and steel have similar specific shear strengths but that CFRP is about 16% better than aluminium alloy. It should be noted that for isotropic materials shear strength is not easily determined. In aluminium alloy tensile failure occurs in a shear mode on the maximum shear stress plane, which is at 45° to the load axis, and the quoted shear strength is usually taken to be half the tensile strength. In the case of steel this type of failure does not occur and for several reasons the shear strength is taken to be $\frac{2}{3}$ of the tensile strength. It is with these values of shear strength that CFRP has been compared.

7.4 Behaviour of multi-hole joints

The results of tests on the multi-hole bolted joints, have shown, with very few exceptions, that there is no adverse interaction between holes and, therefore, no loss in efficiency as the number of holes is increased. For the bolt spacings used, the total load carried by the multi-hole joints, whether single or double rows, was predictable from the single-hole data and it has been demonstrated that multi-hole joints in CFRP could compare favourably with those in other materials.

During tensile tests a reduction in tensile load compared with predicted values was observed for some single-row multi-hole joints but no real explanation has been found. It is, however, possible that poor alignment or poor load distribution between bolts would account for the reduced strength. Because of the constraints on bolt-hole spacing it was not possible to produce shear failures during multi-hole tests and it is not therefore possible to state with certainty that no shear interaction would exist in other situations.

Nonetheless, shear stresses of up to 85 per cent of the predicted shear strengths were achieved during the tests, so that if shear interaction does occur the indications are that it will be small.

7.5 Concluding remarks

Although joint optimisation could be carried out using the data obtained from the tests reported here, further work will be necessary if joint weight is to be fully minimised from a static point of view. In particular the effects of changing bolt-hole spacings and degree of bolt fit in the hole would need to be evaluated. Further work would also need to be done in order to assess the efficiency of CFRP joints from the points of view of fatigue, corrosion, temperature and other environmental effects. Nonetheless, the results presented here are encouraging and serve as a useful pointer to the potential application of mechanical joints to CFRP structural components.

Acknowledgment

The author is much indebted to Mr. A.J. Croucher for the manufacture of the CFRP laminates.

Table 1

SPECIFIC TENSILE STRENGTHS

Material	Tensile strength MN/m^2	Specific gravity g/cc	Specific tensile strength
Steel S96	927	7.85	118
Aluminium alloy L71	432	2.7	160
CFRP (HTS) $0^o \pm 45^o$ $\frac{1}{3}$ $0^o, \frac{2}{3} \pm 45^o$	325	1.54	211

Table 2

SPECIFIC BEARING STRENGTHS

Material	Bearing strength MN/m^2	Specific gravity g/cc	Specific bearing strength
Steel S96	973	7.85	124
Aluminium alloy L71	425	2.7	157
CFRP (HTS) $0^o \pm 45^o$ $\frac{1}{3}$ $0^o, \frac{2}{3} \pm 45^o$	900	1.54	584

Table 3

SPECIFIC SHEAR STRENGTHS

Material	Shear strength MN/m^2	Specific gravity g/cc	Specific shear strength
Steel S96	695	7.85	88
Aluminium alloy L71	216	2.7	80
CFRP (HTS) $0^o \pm 45^o$ $\frac{1}{3}$ $0^o, \frac{2}{3} \pm 45^o$	145	1.54	94

SYMBOLS

A	gross cross-sectional area of laminate
A_0	gross cross-sectional area of 0° laminate in a $0^\circ \pm \alpha^\circ$ laminate
D	lateral clamping pad diameter
d	loaded hole diameter
e	edge distance (distance between hole centre and free edge parallel to applied load)
E_0	Young's modulus of unidirectional CFRP
E_α	Young's modulus of $\pm\alpha^\circ$ CFRP
E_1	principal Young's modulus
E_2	transverse Young's modulus in the plane of the laminate
G	shear modulus
K	torque coefficient
k_{gross}	average gross tensile stress concentration factor
k_{net}	average net tensile stress concentration factor
$L_{(ult)}$	failing load
ℓ	bolt pitch
n	number of holes occurring across a specimens cross section
P	total load carried by a laminate
P_0	load carried by 0° fibres in a laminate
P_t	tensile load in a bolt due to torque tightening
$P_{(ult)}$	ultimate load carried by a laminate
$P_{0(ult)}$	ultimate load carried by 0° fibres in a laminate
t	total thickness of a laminate (joint thickness)
t_0	thickness of 0° laminate in a $0^\circ \pm \alpha^\circ$ laminate
t	thickness of α° laminate in a $0^\circ \pm \alpha^\circ$ laminate
T	torque applied to loading pins (bolts)
v_f	fibre volume fraction
W	specimen width
$W_{(d)}$	joint weight
α	orientation of laminate to principal direction
$\varepsilon_{(d)}$	joint efficiency
θ	angle subtended from load axis line on the compression face of the loaded hole
ν_{12}	principal Poissons ratio
$\sigma_{net(ult)}$	net tensile stress at failure
$\sigma_{gross(ult)}$	gross tensile stress at failure

SYMBOLS (concluded)

$\sigma_{f(ult)}$	tensile strength of fibre
$\sigma_{x(ult)}$	tensile failing stress of an unpierced laminate
$\sigma_{b(ult)}$	ultimate bearing strength
σ_z	lateral clamping pressure at loaded hole
$\tau_{xy(ult)}$	ultimate shear strength
x (suffix)	laminate in-plane axes
y (suffix)	
z (suffix)	axis normal to plane of laminate

REFERENCES

No.	Author	Title, etc.
1	R. Ulbricht	Filament wound glass reinforced pressure vessels. Presented as Paper 15 at the Plastic Institutes Filament Winding Conference (1967)
2	P.E. Gallant M.W. Jones	Development of a helically wound rocket motor case. Presented as Paper 13 at the Plastic Institutes Filament Winding Conference (1967)
3	E.E. Morris R.J. Alfring	Cryogenic boron filament wound pressure vessels. Composite Materials: Testing and Design ASTM STP 460 (1969)
4	D.M. McElhinney A.W. Kitchenside K.A. Rowland	The use of carbon fibre reinforced plastics. Aircraft Engineering, October 1969
5	G. Lubin W. Ludwig A. August	Boron wing extension for F-1 11B aircraft. From Proceedings of SPE 26th Annual Conference (1968)
6	R.N. Hadcock	Design philosophy for boron/epoxy structures. Composite Materials: Testing and Design ASTM STP 497 (1972)
7	H.E. Gresham	The development of fibre reinforced composites for gas turbines. Inst. of Prod. Engineers, May 1969
8	H.F. Winny	The use of carbon fibre composites in helicopters. The Aeronautical Journal, Volume 75, No.732, December 1971
9	J. Fray	A carbon fibre Vulcan airbrake flap. The Aeronautical Journal, Volume 75, No.732, December 1971
10	R.C. Sanders	The effect of carbon fibre composites on design. The Aeronautical Journal, Volume 75, No.732, December 1971

REFERENCES (continued)

No.	Author	Title, etc.
11	T.A. Collings	Design development of an aircraft strut in carbon fibre reinforced plastic. Aeronautical Research Council Current Paper 1229 (1972)
12	M. Goland N.Y. Buffalo E. Reissner	The stresses in cemented joints. Paper Presented at the Annual Meeting of ASME (1943)
13	K.R. Berg	Analysis of axial stresses in a multi-ply laminate loaded in shear on the outer-ply. Whittaker Corporation, Narmco Research and Development Division Technical Note 67-TN-61, April 1967
14	R.N. Dallas	Methods of joining advanced fibrous composites. Composite Materials: Testing and Design, ASTM STP 460 (1969)
15	F. Clifton D.L. Mead	The strength of sheets and joints in unwoven glass fibre reinforced plastic laminates. RAE Technical Report 70213 (1970)
16	J.B. Sturgeon	Joints in carbon fibre reinforced plastics: bonded and bolted joints (2). MOD (PE) unpublished work
17	Rotorway Components Ltd.	CFRP laminate fatigue tests. Technical Note 27, April 1970
18	H.C. Schjelderup B.H. Jones	Practical influence of fibrous reinforced composites in aircraft structural design. Composite Materials: Testing and Design ASTM STP 460 (1969)
19	G.A. Clark K.I. Clayton	Fabrication techniques for advanced composite attachments and joints. North American Rockwell Corporation Technical Report AFML-TR-69-151, May 1969

REFERENCES (continued)

No.	Author	Title, etc.
20	J.P. Wong B.W. Cole A.L. Courtney	Development of the shim joint concept for composite structural members. Technical Report AFFDL-TR-67-116, August 1967
21	G.E. Padawer	The strength of bolted connections in graphite/epoxy composites reinforced by colimated boron film. Composite Materials: Testing and Design ASTM STP 497 (1972)
22	J.E. Ashton M.L. Burdorf F. Olson	Design analysis, and testing of an advanced composite F 111 fuselage. Composite Materials: Testing and Design ASTM STP 497 (1972)
23	G.M. Lehman A.V. Hawley, *et al.*	Investigation of joints in advanced fibrous composites for aircraft structures. Technical Report AFFDL-TR-69-43, Volumes 1 and 2, June 1969
24	Sarah M. Bishop	Stresses near an elliptical hole in an orthotropic sheet. RAE Technical Report 72026 (1972)
25	C.H. Holleman	Tension joints in aircraft structures. Journal of Aeronautics Sciences, Volume 10, p.295, October 1943
26	T.A. Collings P.D. Ewins	Unpublished work
27	P.D. Ewins	A compressive test specimen for unidirectional carbon fibre reinforced plastics. RAE Technical Report 70007 (1970)
28	-	Procurement Executive of the Ministry of Defence Provisional Specification NM 565
29	-	Procurement Executive of the Ministry of Defence Provisional Specification NM 547

REFERENCES (continued)

No.	Author	Title, etc.
30	T.A. Collings P.D. Ewins	Tensile and compressive strength measurements on some unidirectional carbon fibre reinforced plastics. RAE Technical Report 72063 (1972)
31	W.C. Stewart	Metals engineering design. ASME Handbook, Second Edition, p.331 (1965)
32	-	British Standard BS 164 (1941)
33	-	British Standard BS 1916 (1953)
34	P.D. Ewins	Tensile and compressive test specimens for unidirectional carbon fibre reinforced plastics. RAE Technical Report 71217 (1971)
35	J.B. Sturgeon	Specimens and test methods for carbon fibre reinforced plastics. RAE Technical Report 71026 (1971)
36	M.B. Snell	Report to be published
37	M.E. Waddoups J.R. Eisemann B.E. Kaminski	Macroscopic fracture mechanics of advanced composite materials. Journal of composite materials, Volume 5, p.446, October 1971
38	S.G. Lekhnitski	Anisotropic plates. 2nd Edition, p.171, Gordon and Breach (1968)
39	S.V. Kulkarni B.W. Rosen C. Zweben	Load concentration factors for circular holes in composite laminates. Journal of Composite Materials, Volume 7, p.387, July 1973
40	D.L. Mead	The strength and stiffness in transverse tension of unidirectional carbon fibre reinforced plastic. RAE Technical Report 72129 (1972)
41	W.G. Bickley	Philosophical transactions of the Royal Society of London, Series A. Volume 227, p.399 (1928)

REFERENCES (concluded)

No.	Author	Title, etc.
42	M.M. Frocht H.N. Hill	Stress concentration factors around a central circular hole in a plate loaded through pin in the hole. Transactions of the American Society of Mechanical Engineers, Journal of Applied Mechanics, Volume 17, p.A5 (1940)
43	J.P. Waszczak T.A. Cruse	A synthesis procedure for mechanically fastened joints in advanced composite materials. AD-771795, September 1973

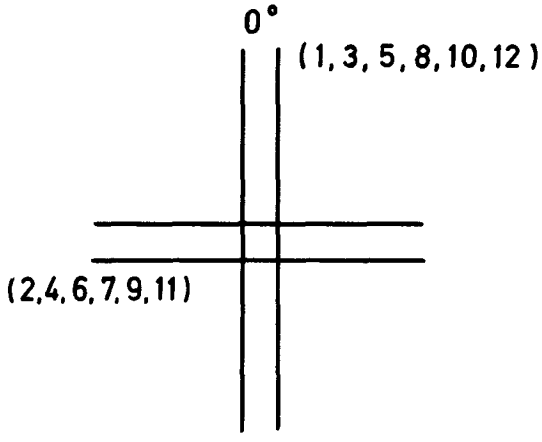

a $0°/90°$

$\frac{1}{2}\ 0°\quad \frac{1}{2}\ 90°$

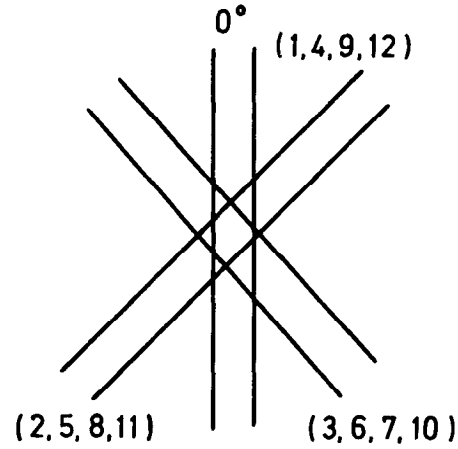

b $0° \pm 45°$

$\frac{1}{3}\ 0°\quad \frac{2}{3}\ \pm 45°$

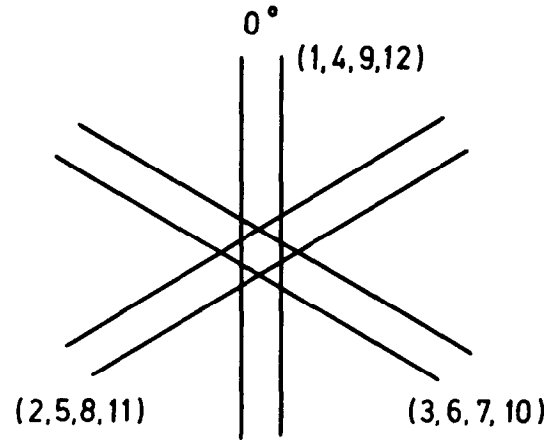

c $0° \pm 60°$

$\frac{1}{3}^{\circ}\ 0°\quad \frac{2}{3}^{\circ}\ \pm 60°$

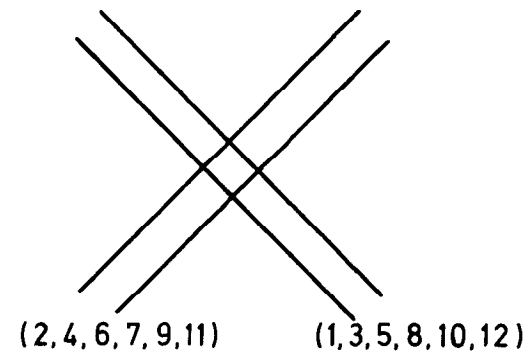

d $\pm 45°$

Fig.1a&b Stacking sequence for 12 ply laminates

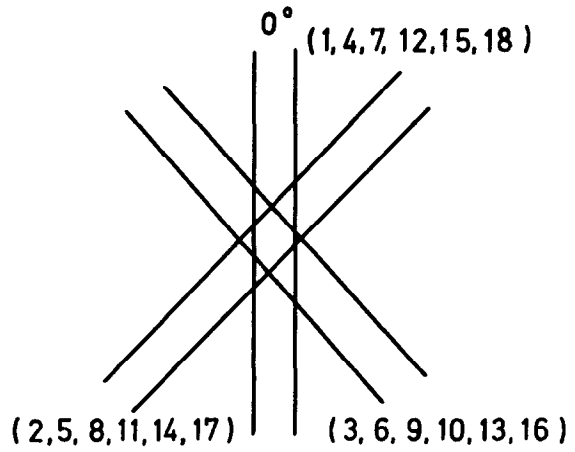

a $0° \pm 45°$ 18 ply laminate

$\frac{1}{3}\,0° \quad \frac{2}{3} \pm 45°$

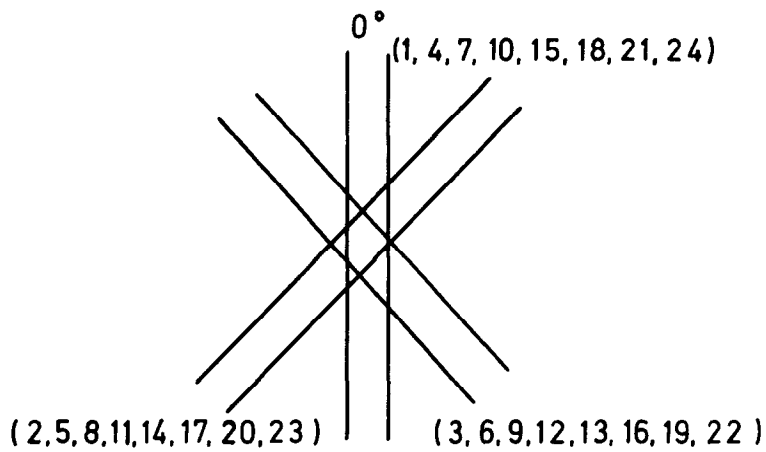

b $0° \pm 45°$ 24 ply laminate

$\frac{1}{3}\,0° \quad \frac{2}{3} \pm 45°$

Fig.2a&b Stacking sequences for 18 and 24 ply laminates

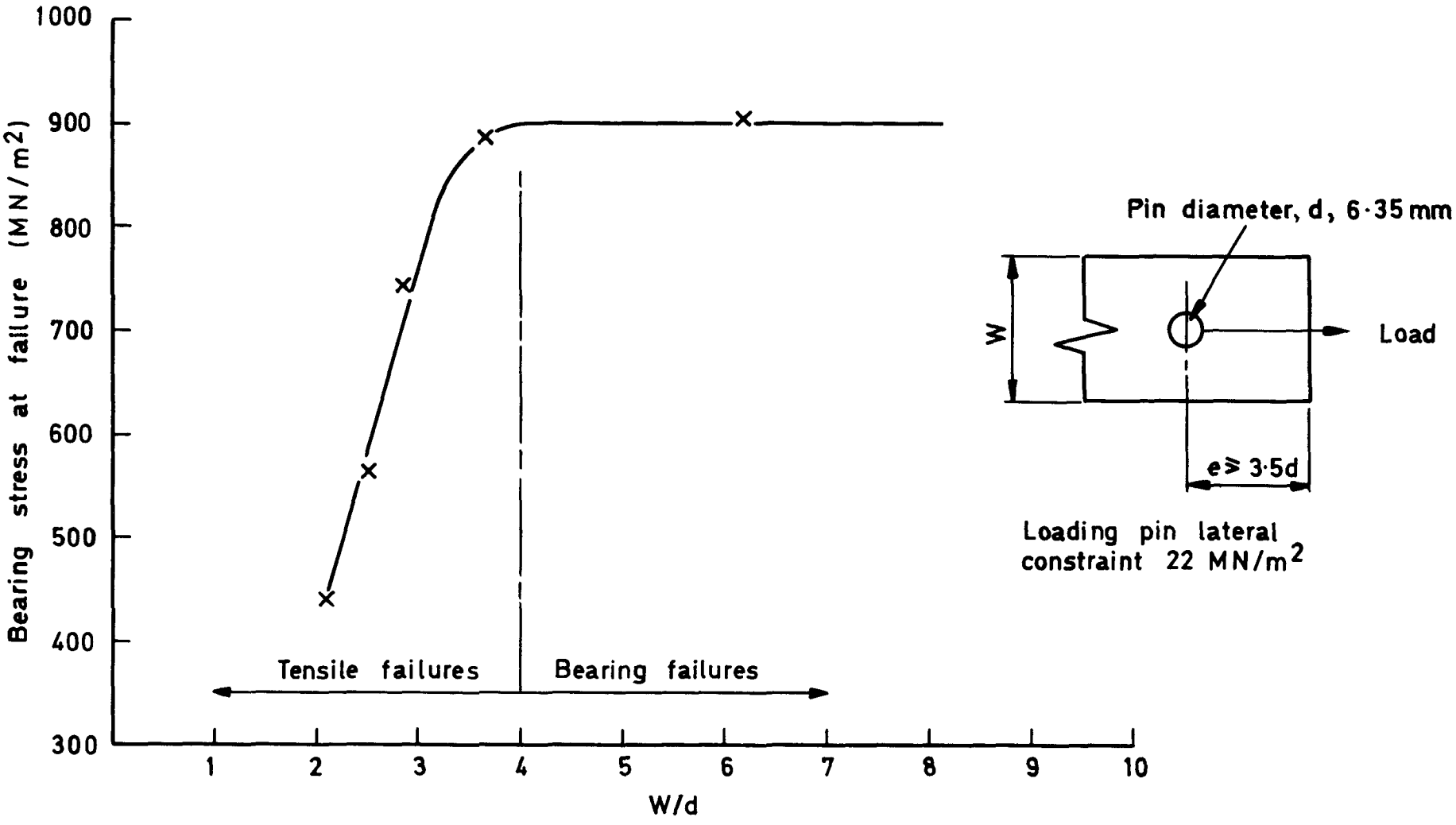

Fig.3 Variation of bearing stress at failure with W/d ratio (0° ± 45° laminate)

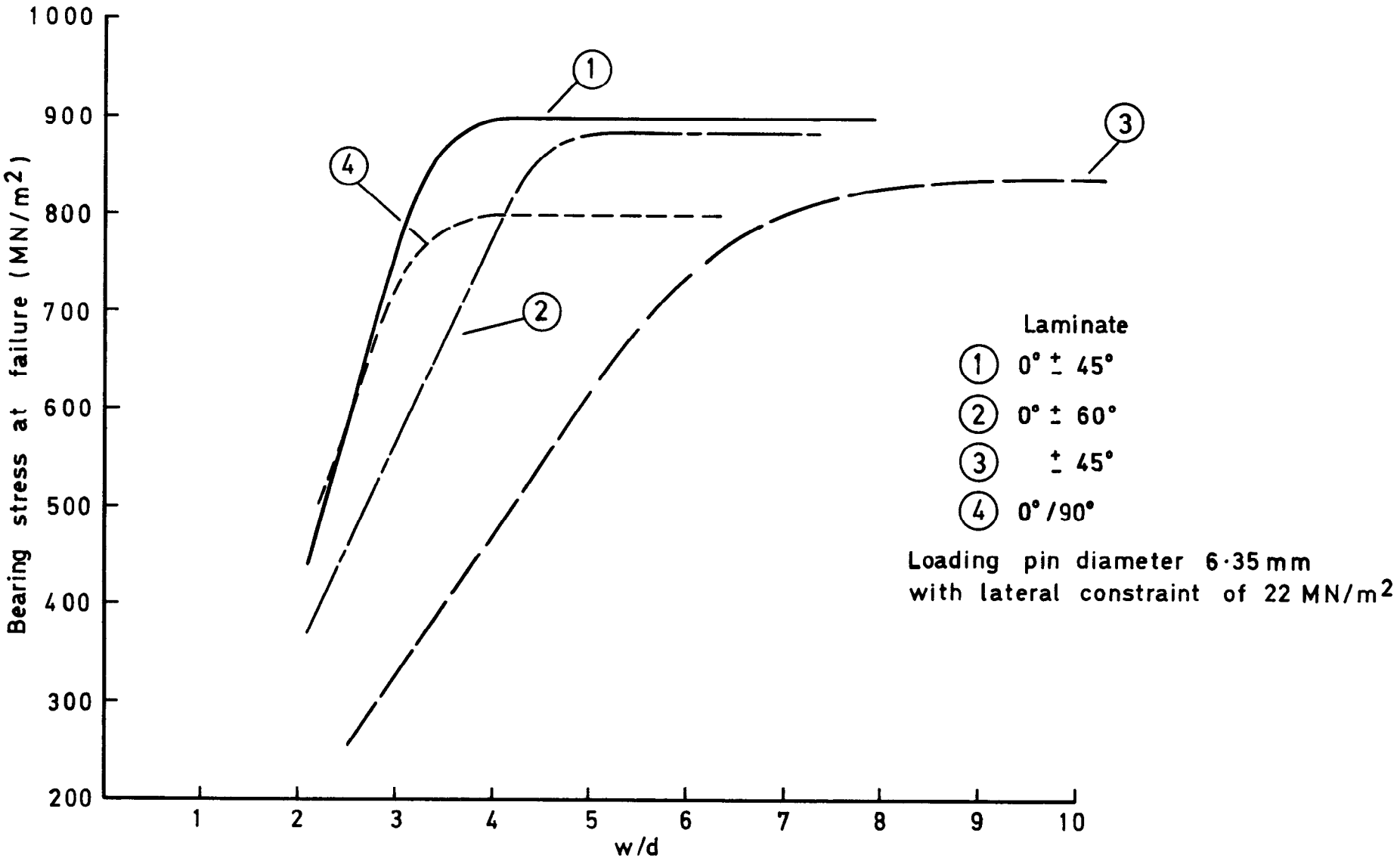

Fig. 4 Variation of bearing stress at failure with W/d ratio (various laminates)

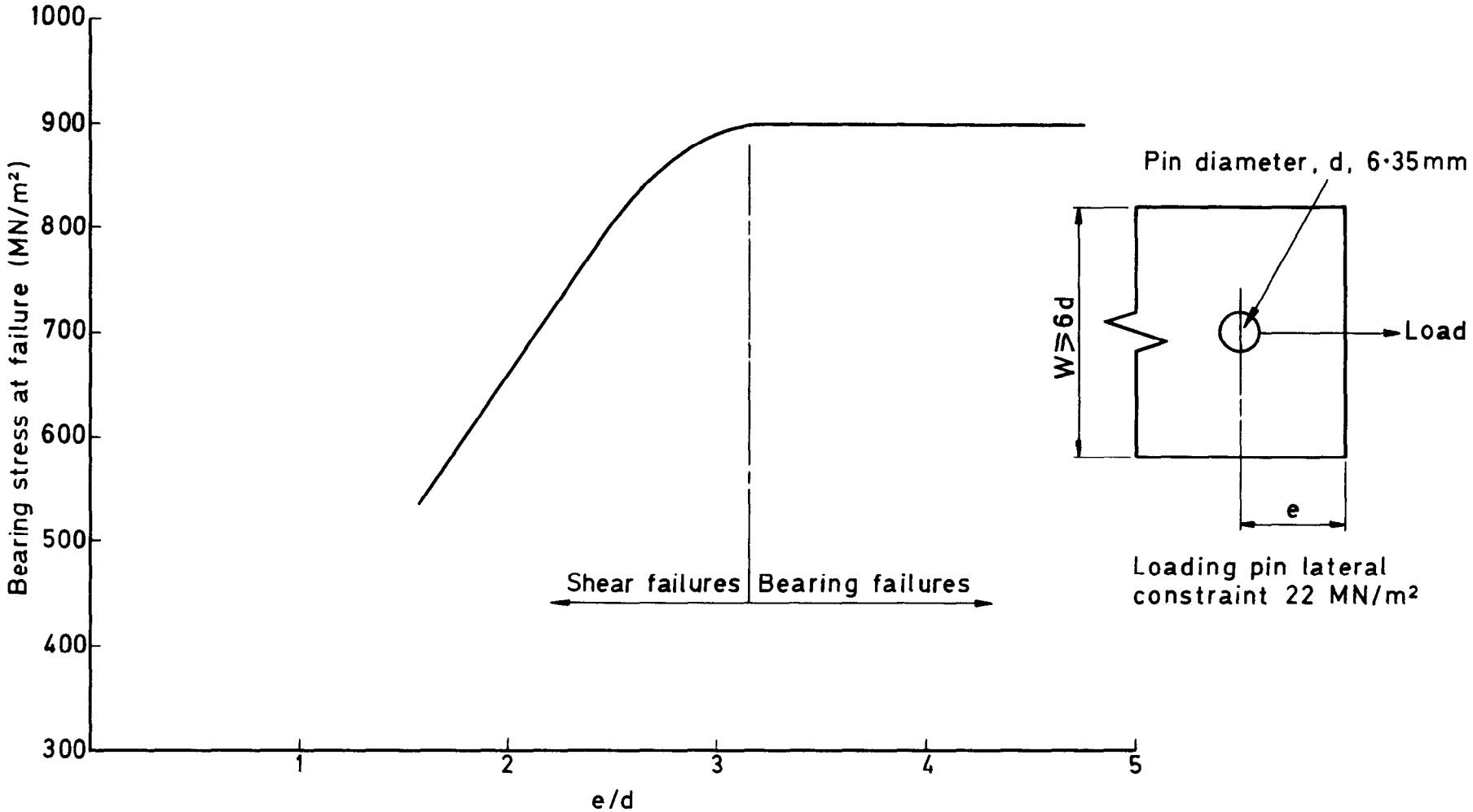

Fig. 5 Variation of bearing stress at failure with e/d ratio (0° ±45° laminate)

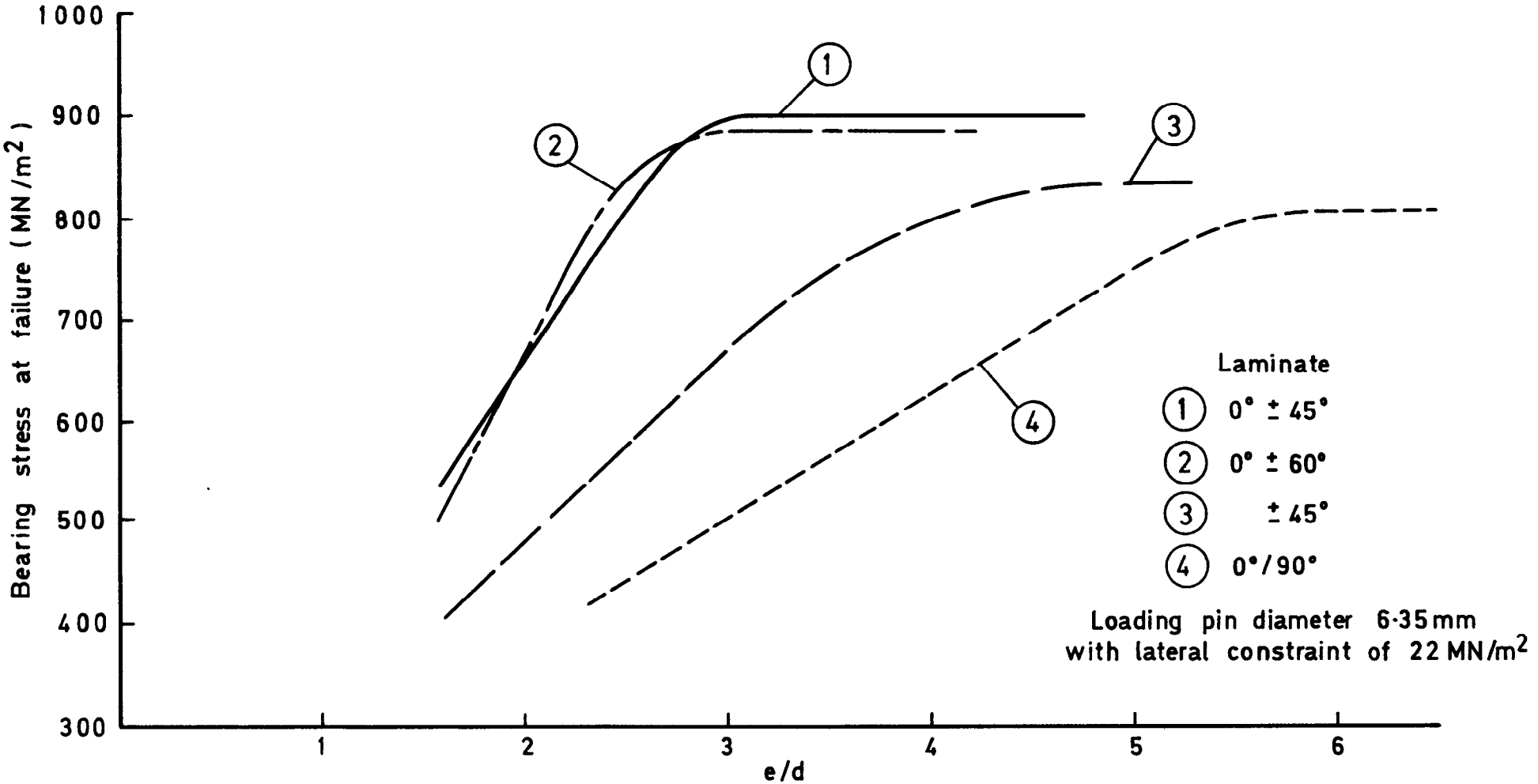

Fig. 6 Variation of bearing stress at failure with e/d ratio (various laminates)

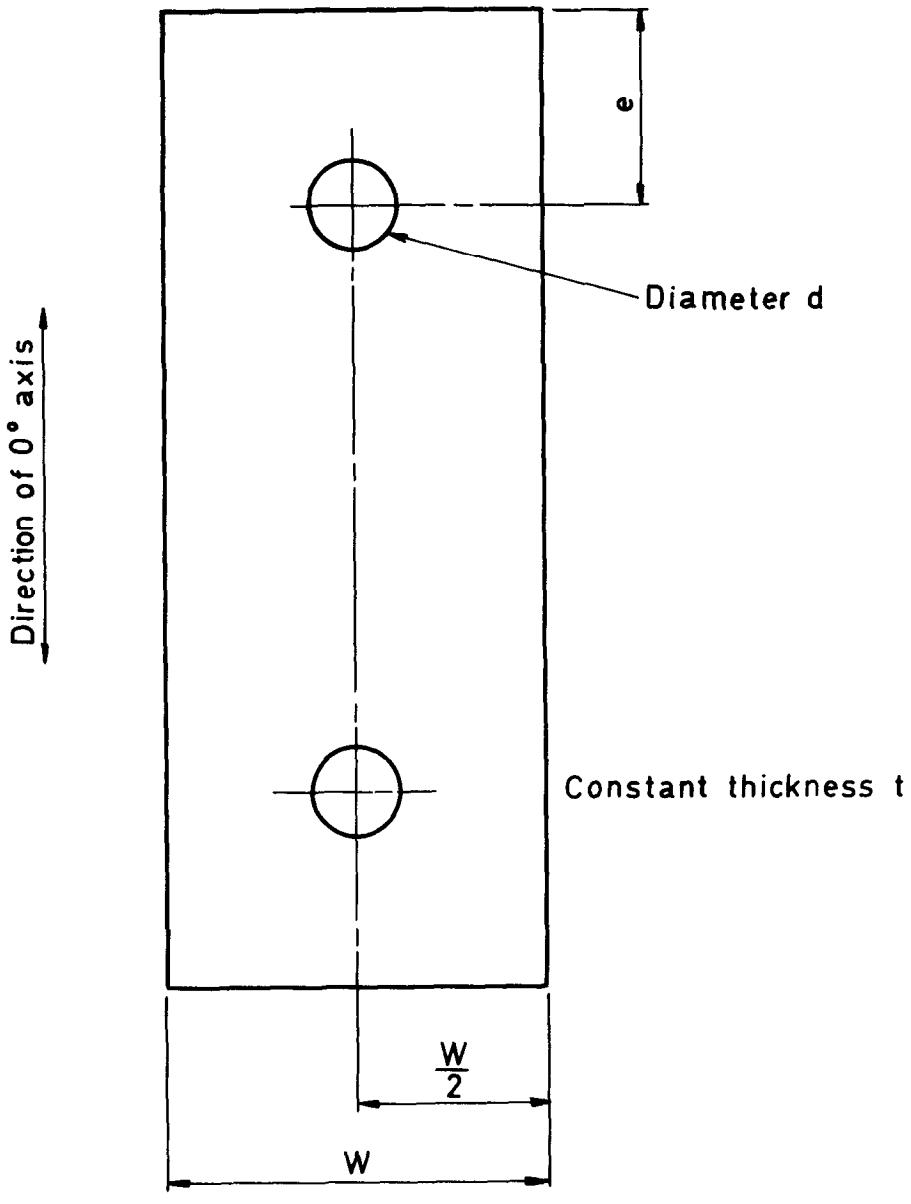

Fig.7 Test specimen

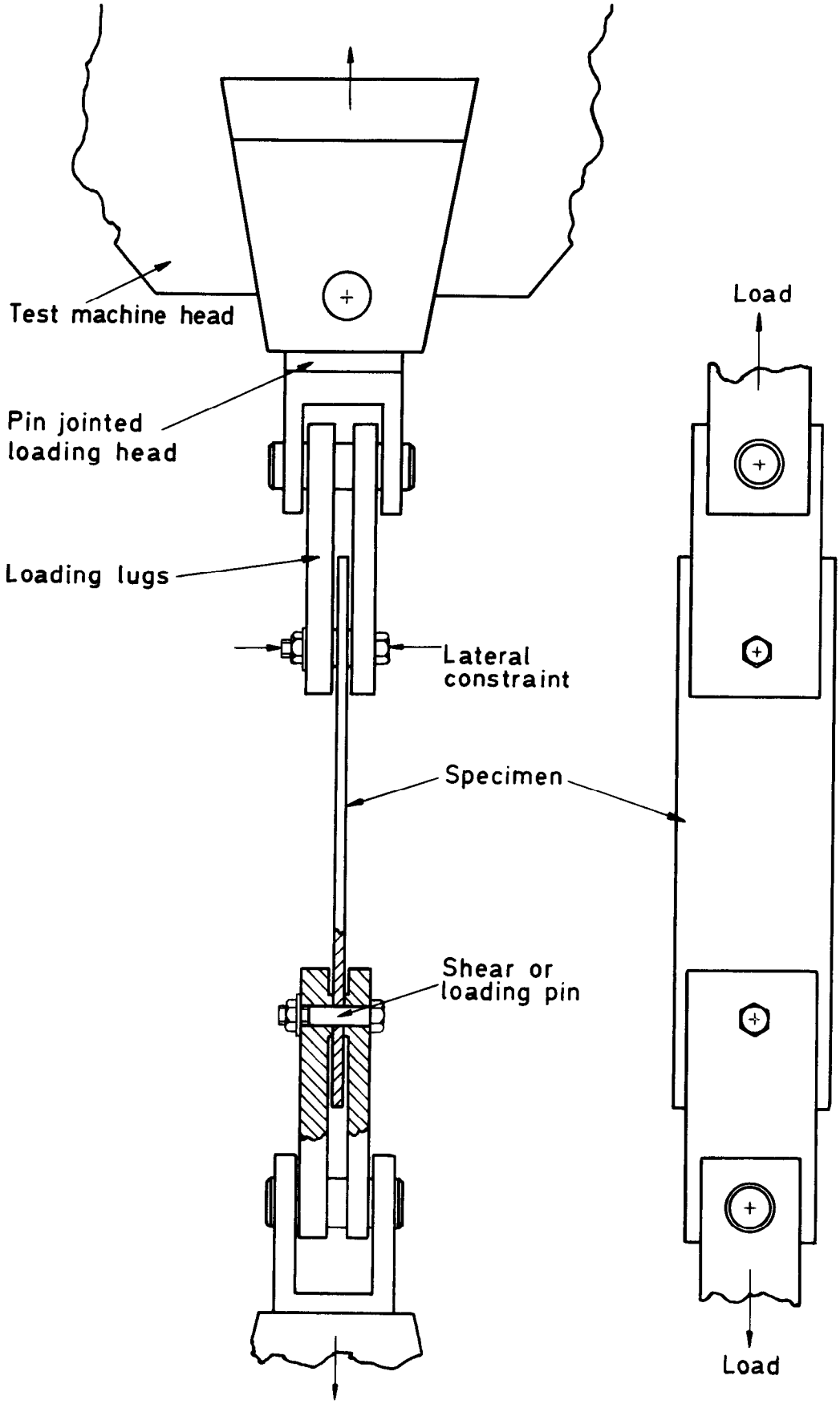

Fig.8 Loading of test specimens

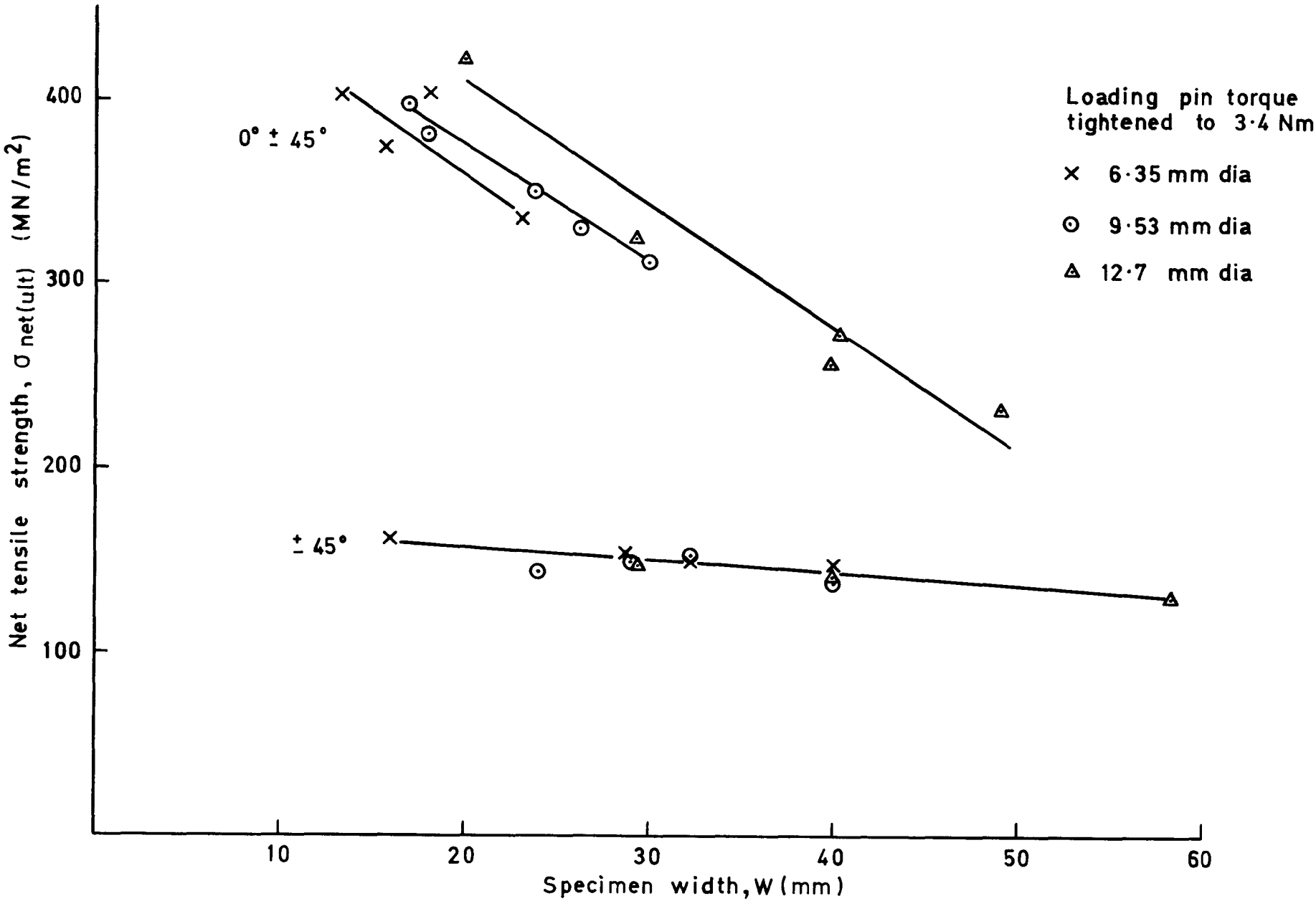

Fig.9 Variation of net tensile strength with specimen width (± 45° and 0° ± 45° laminates)

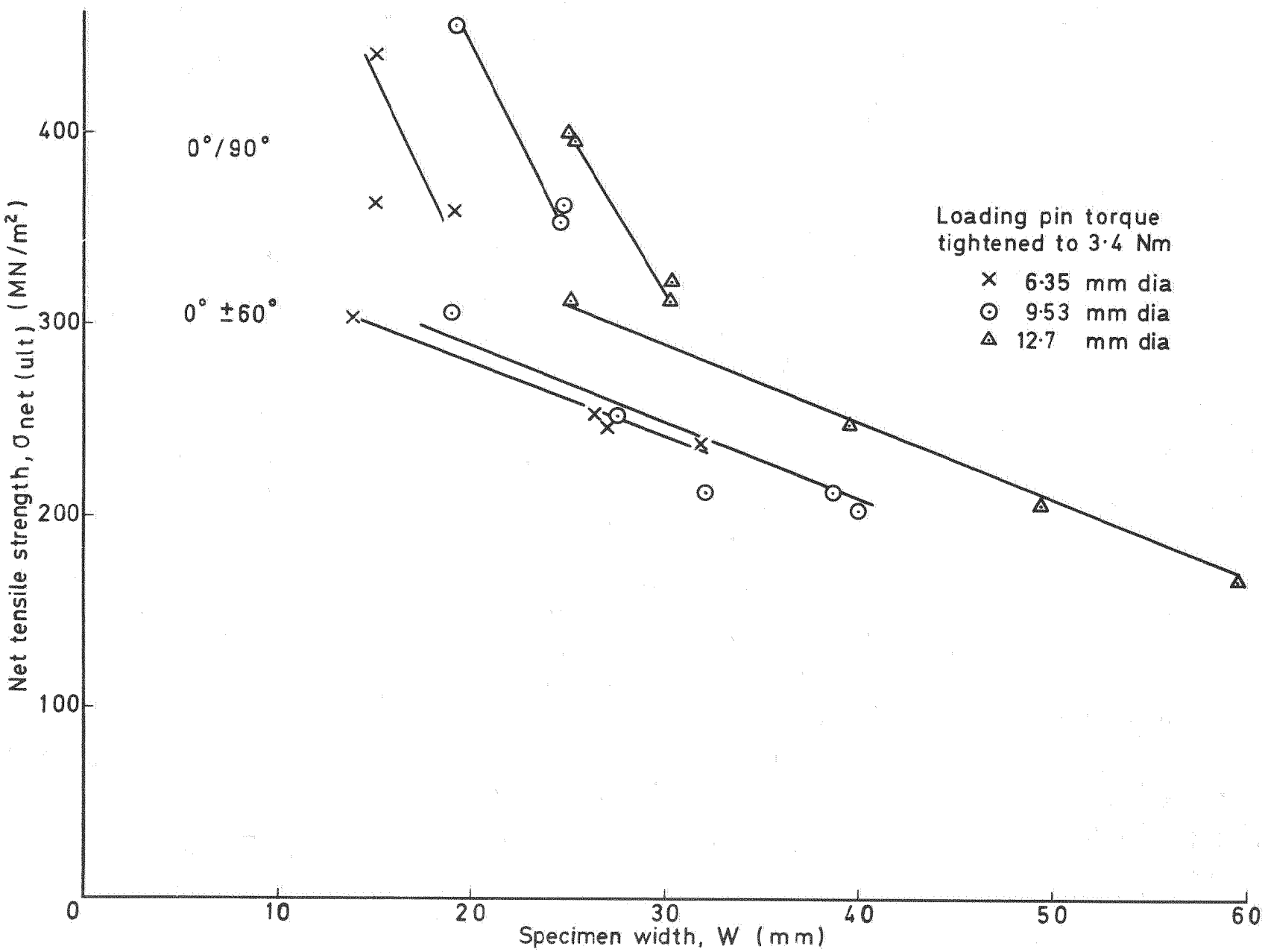

Fig. 10 Variation of net tensile strength with specimen width (0°/90° and 0° ±60° laminates)

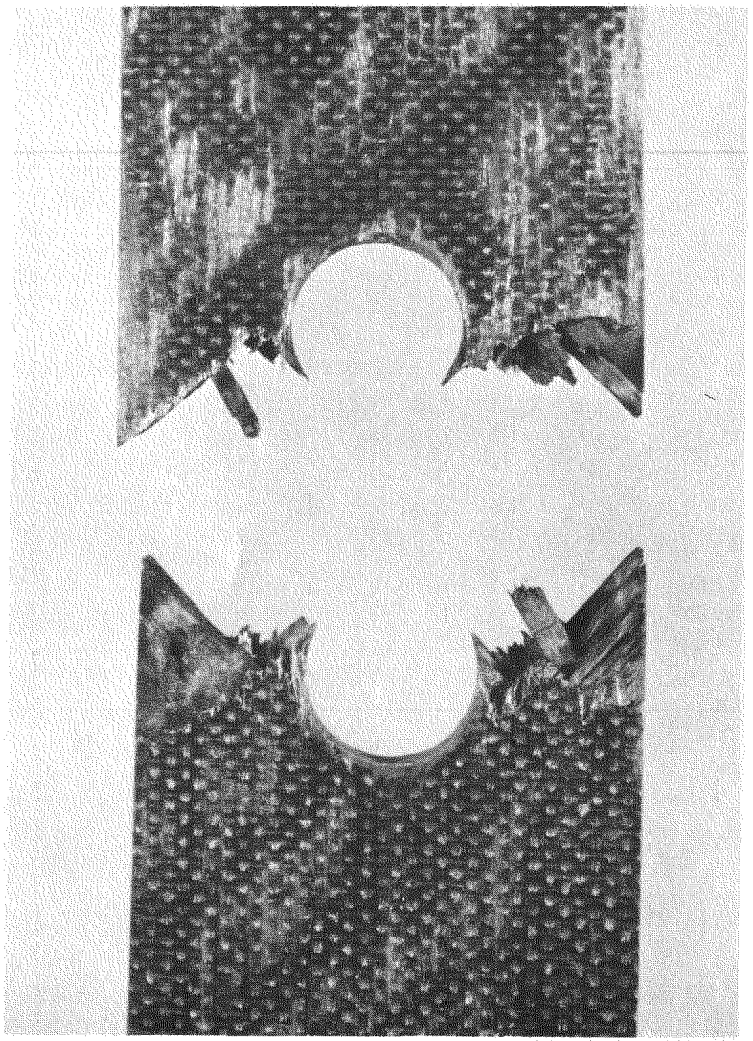

a. $0^\circ \pm 45^\circ$ laminate

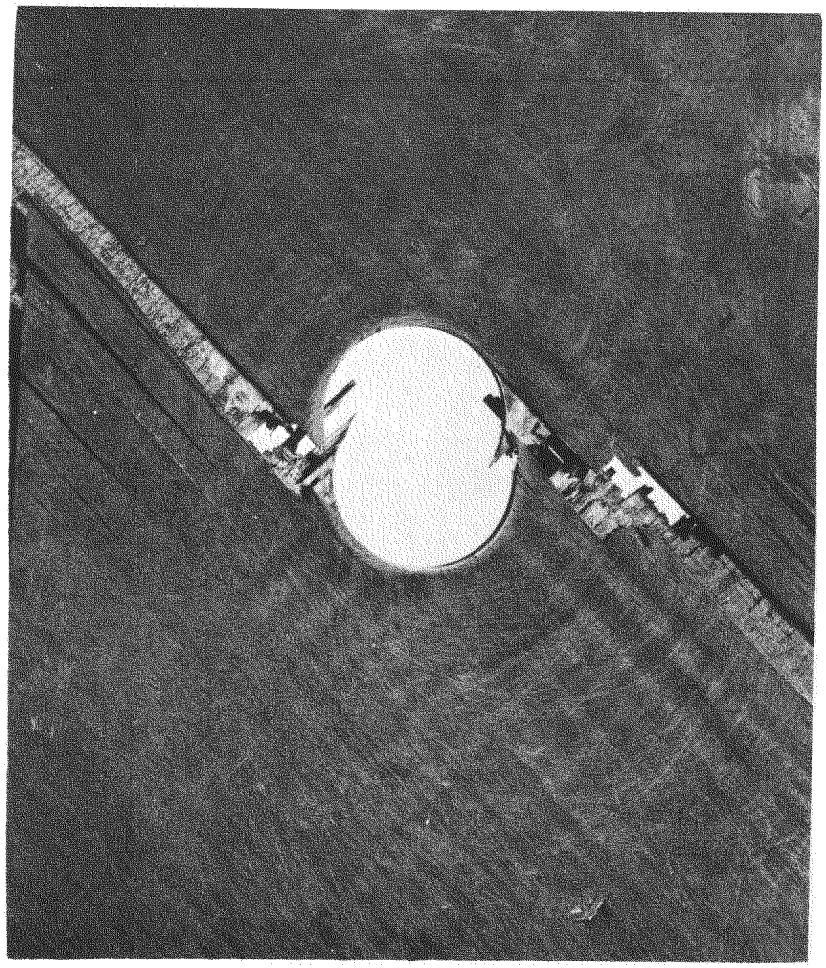

b. $\pm 45^\circ$ laminate

Fig.11a & b Tensile failures

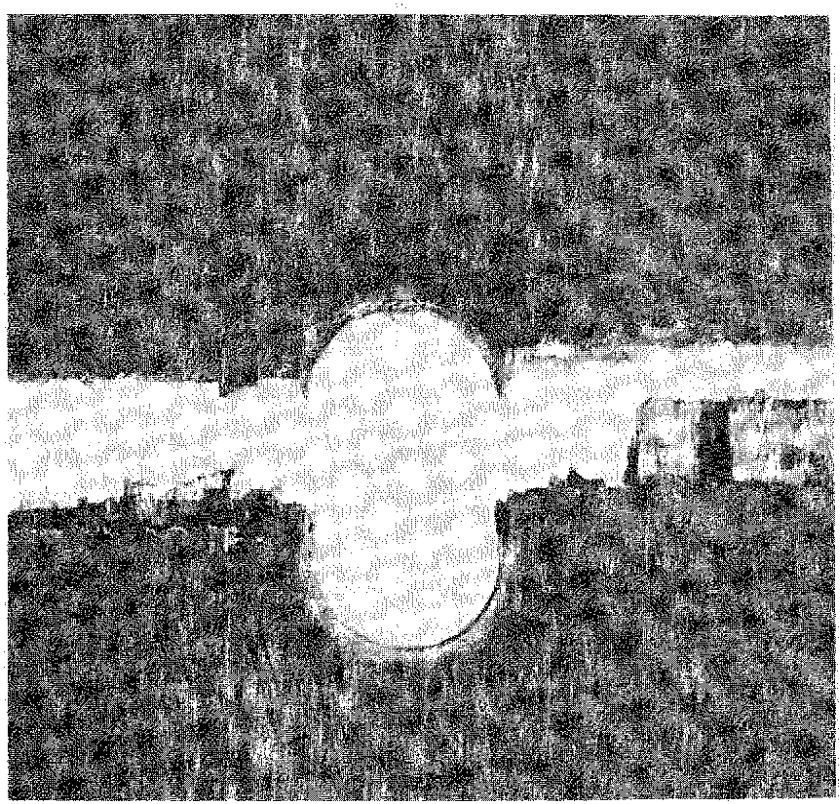

c. $0^{\circ}/90^{\circ}$ laminate

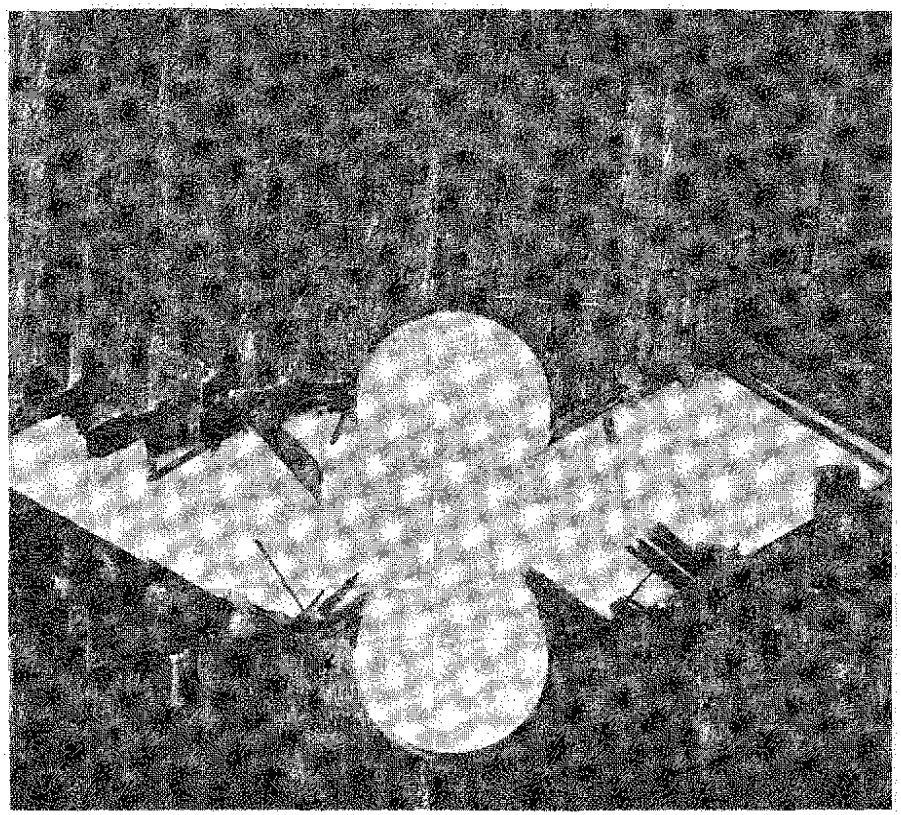

d. $0^{\circ} \pm 60^{\circ}$ laminate

Fig.11c & d Tensile failures

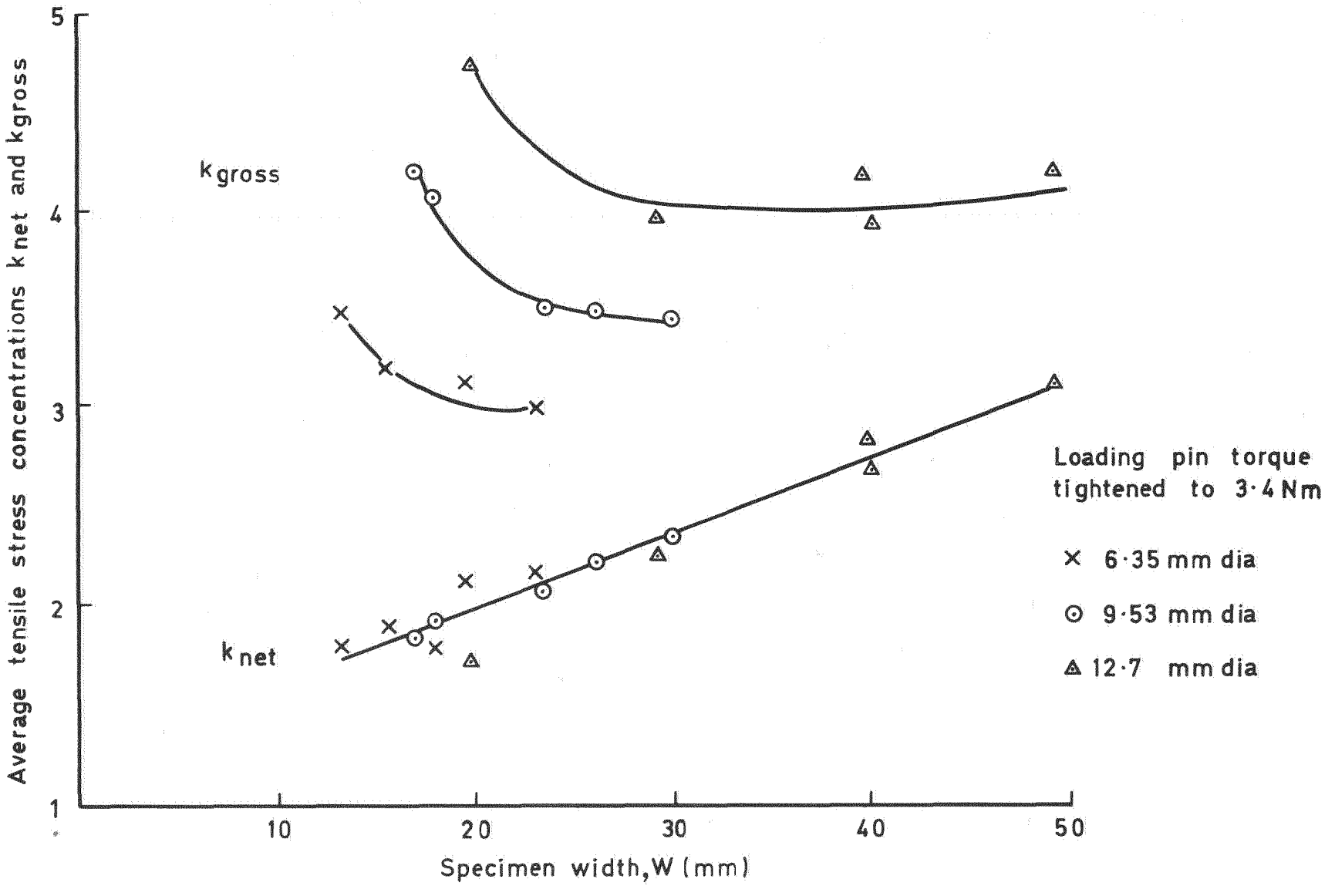

Fig .12 Average tensile stress concentration factors ($0^{\circ} \pm 45^{\circ}$ laminate)

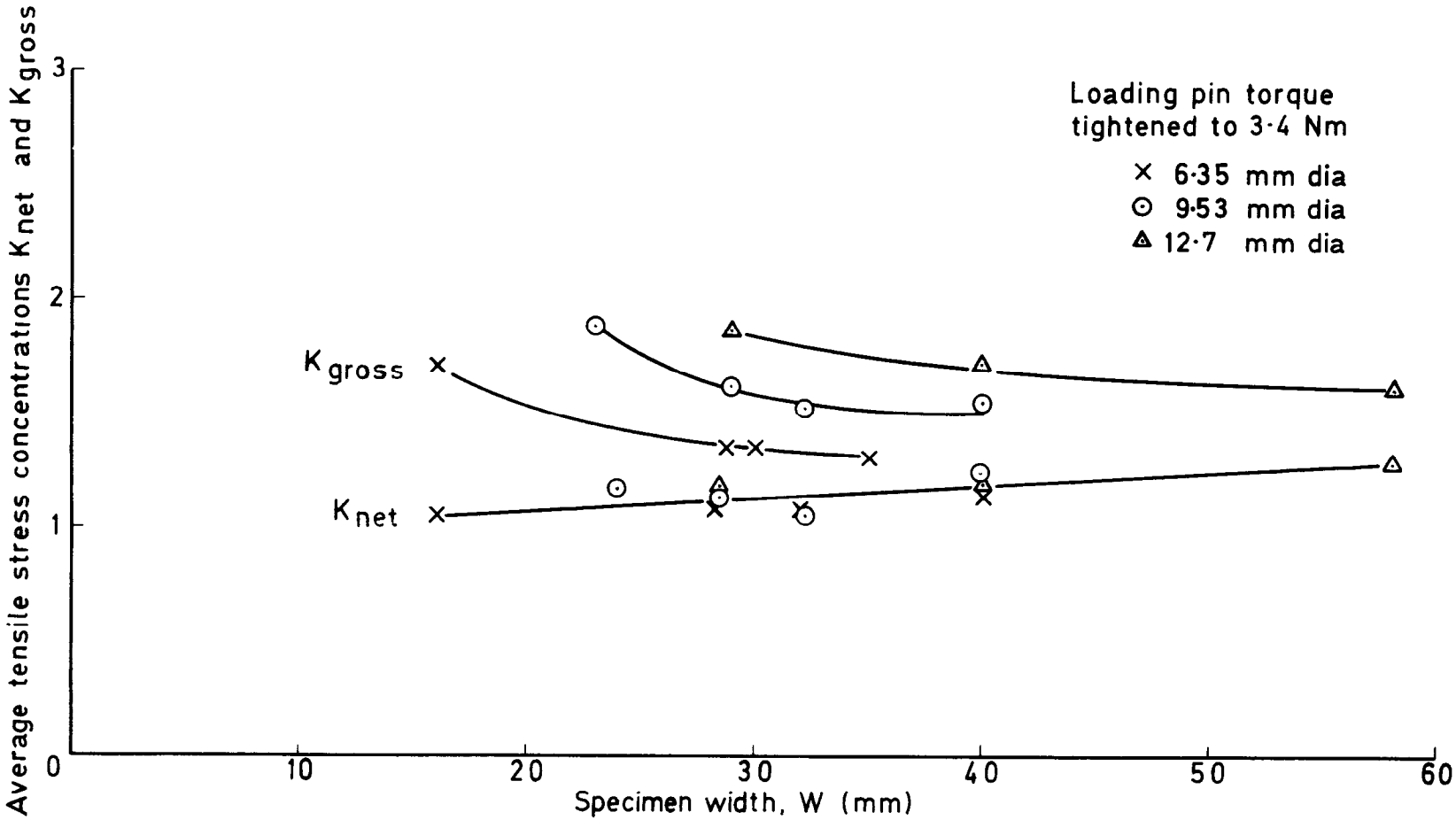

Fig.13 Average tensile stress concentration factors (±45° laminate)

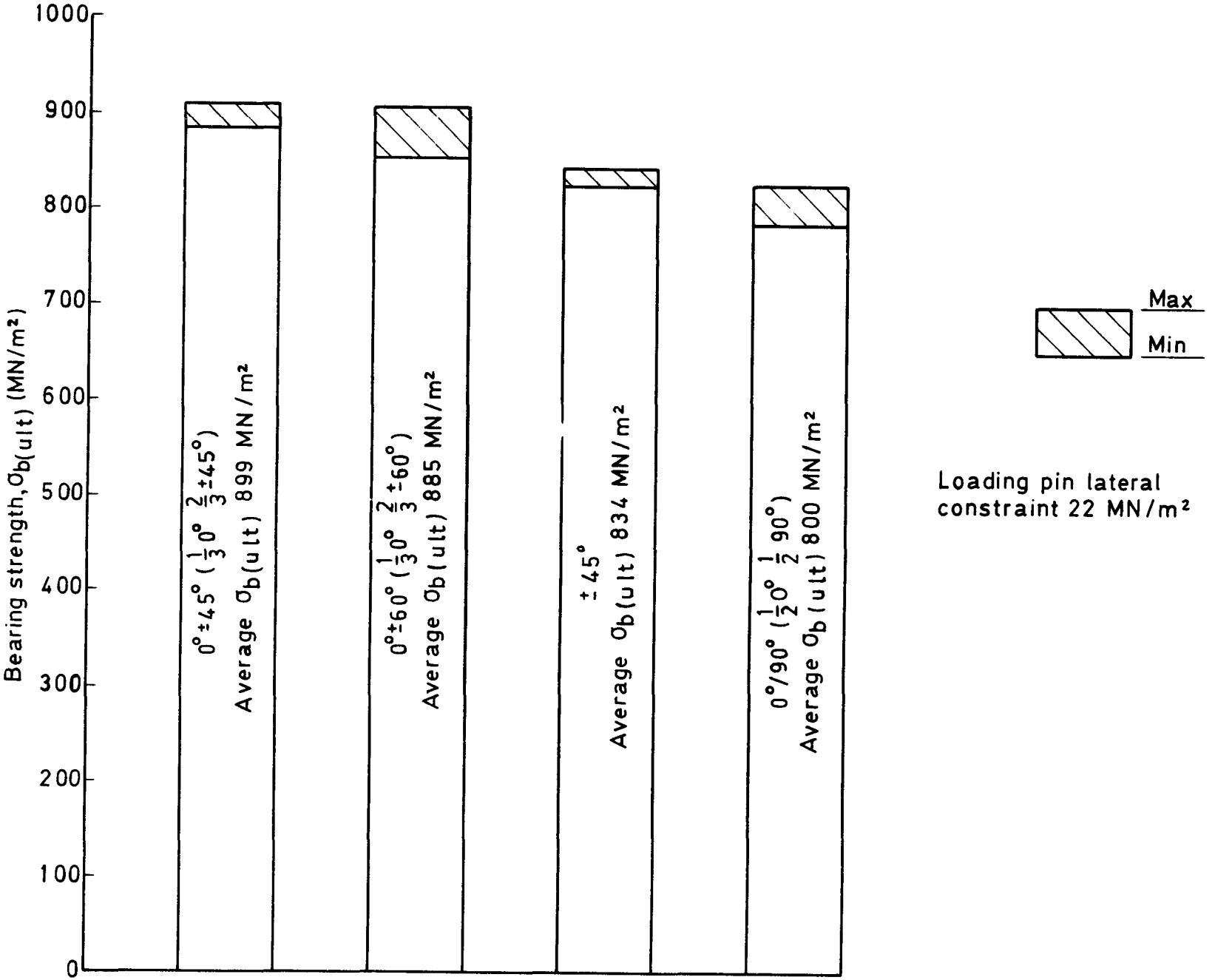

Fig. 14 Effect of fibre orientation on bearing strength (6·35mm diameter hole)

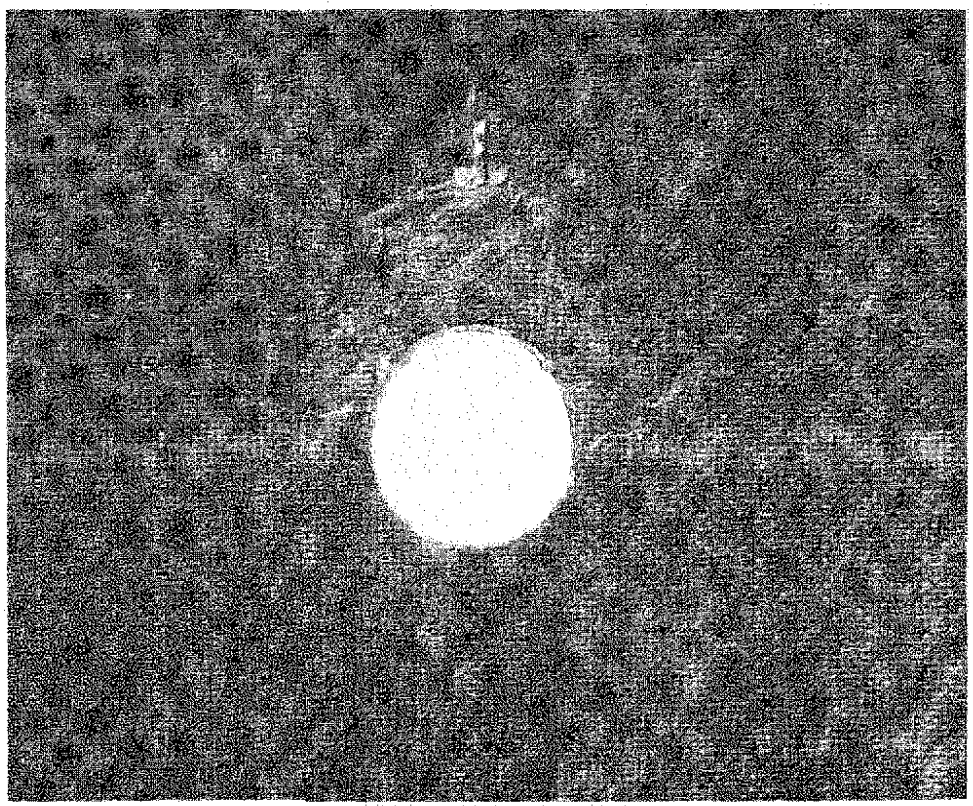

a. $0^{\circ} \pm 45^{\circ}$ laminate

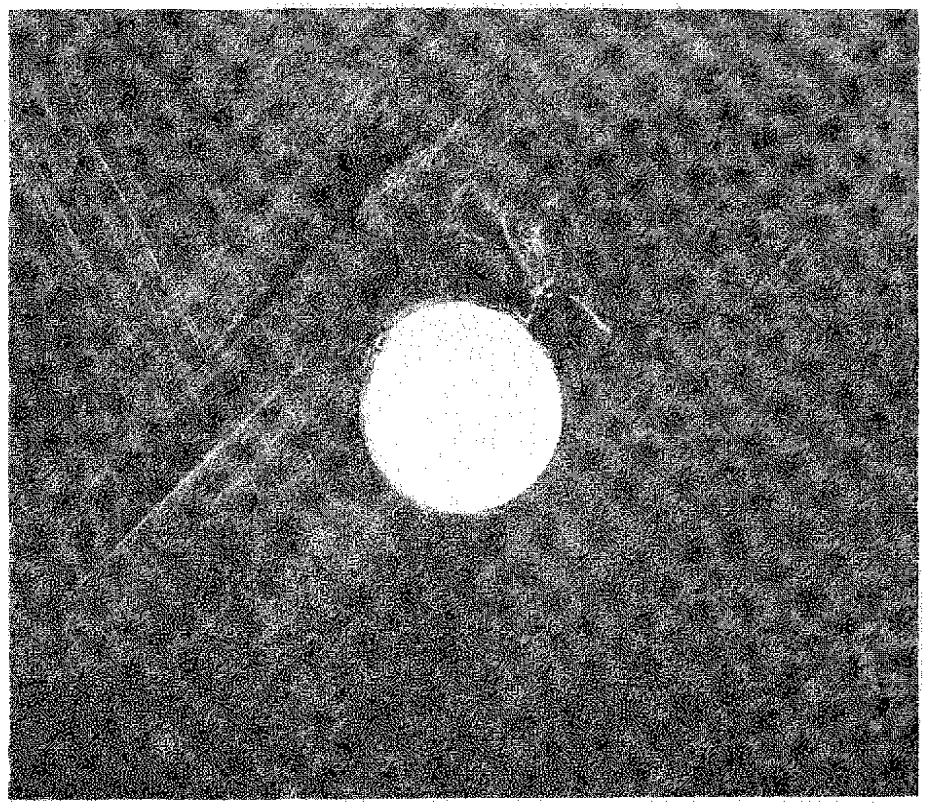

b. $\pm 45^{\circ}$ laminate

Fig.15a & b Bearing failures (constrained laterally)

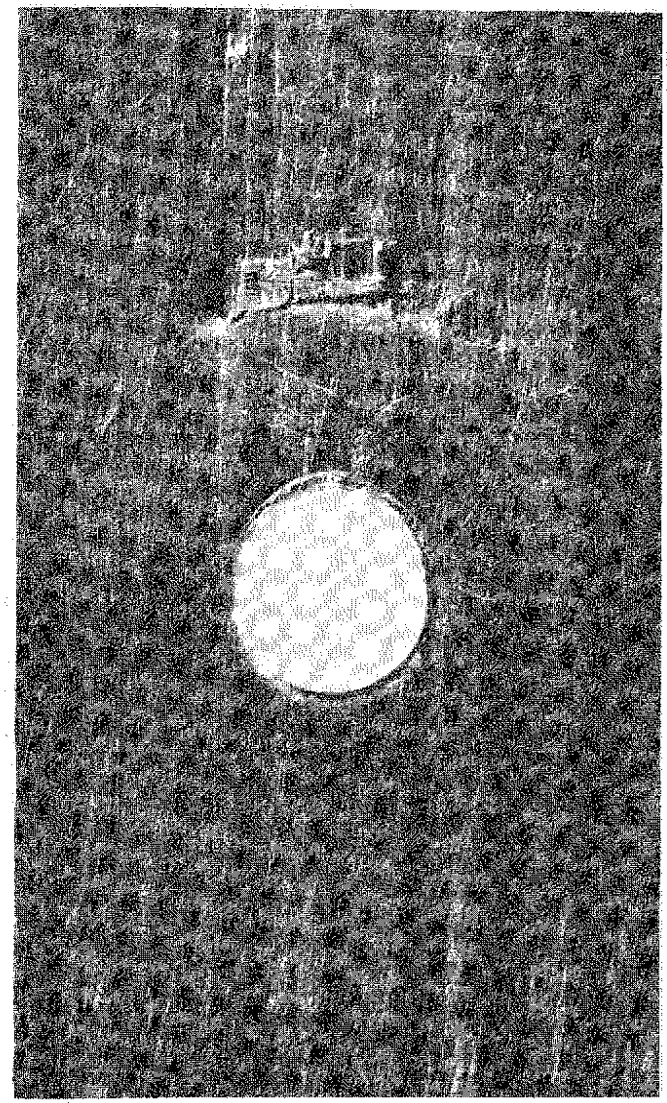

c. $0^{\circ}/90^{\circ}$ laminate

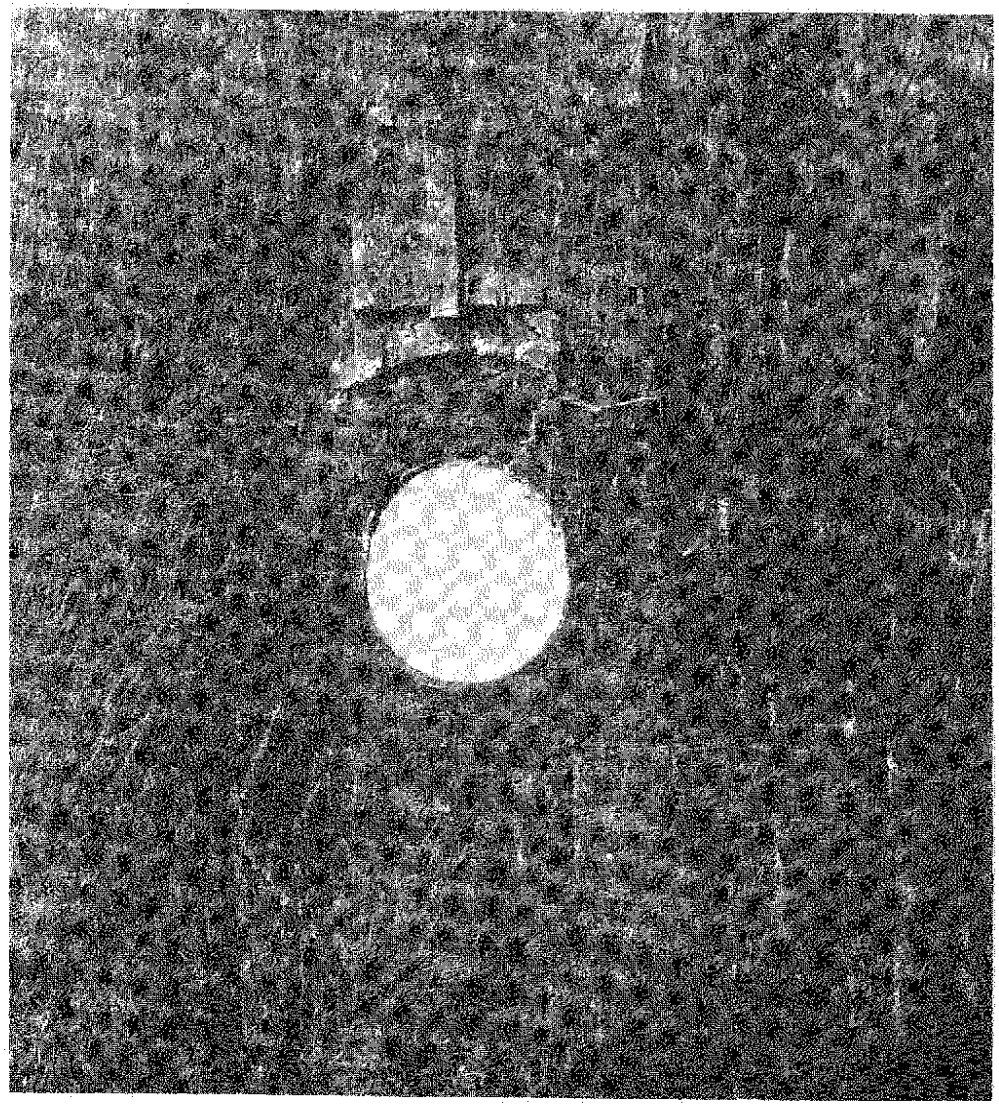

d. $0^{\circ} \pm 60^{\circ}$ laminate

Fig.15c & d Bearing failures (constrained laterally)

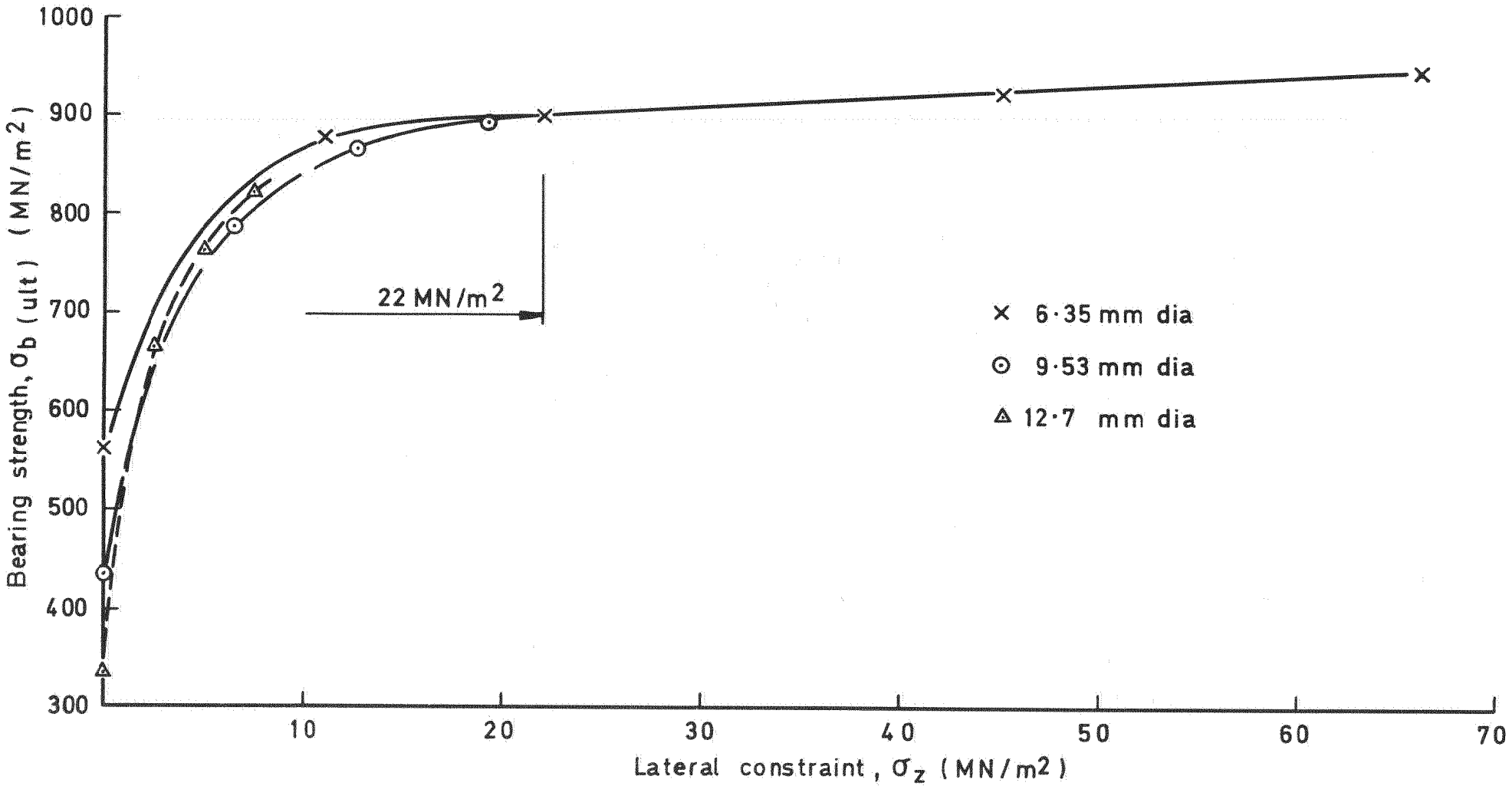

Fig.16 Variation of bearing strength with lateral constraint (various hole diameters, 0° ± 45° laminate)

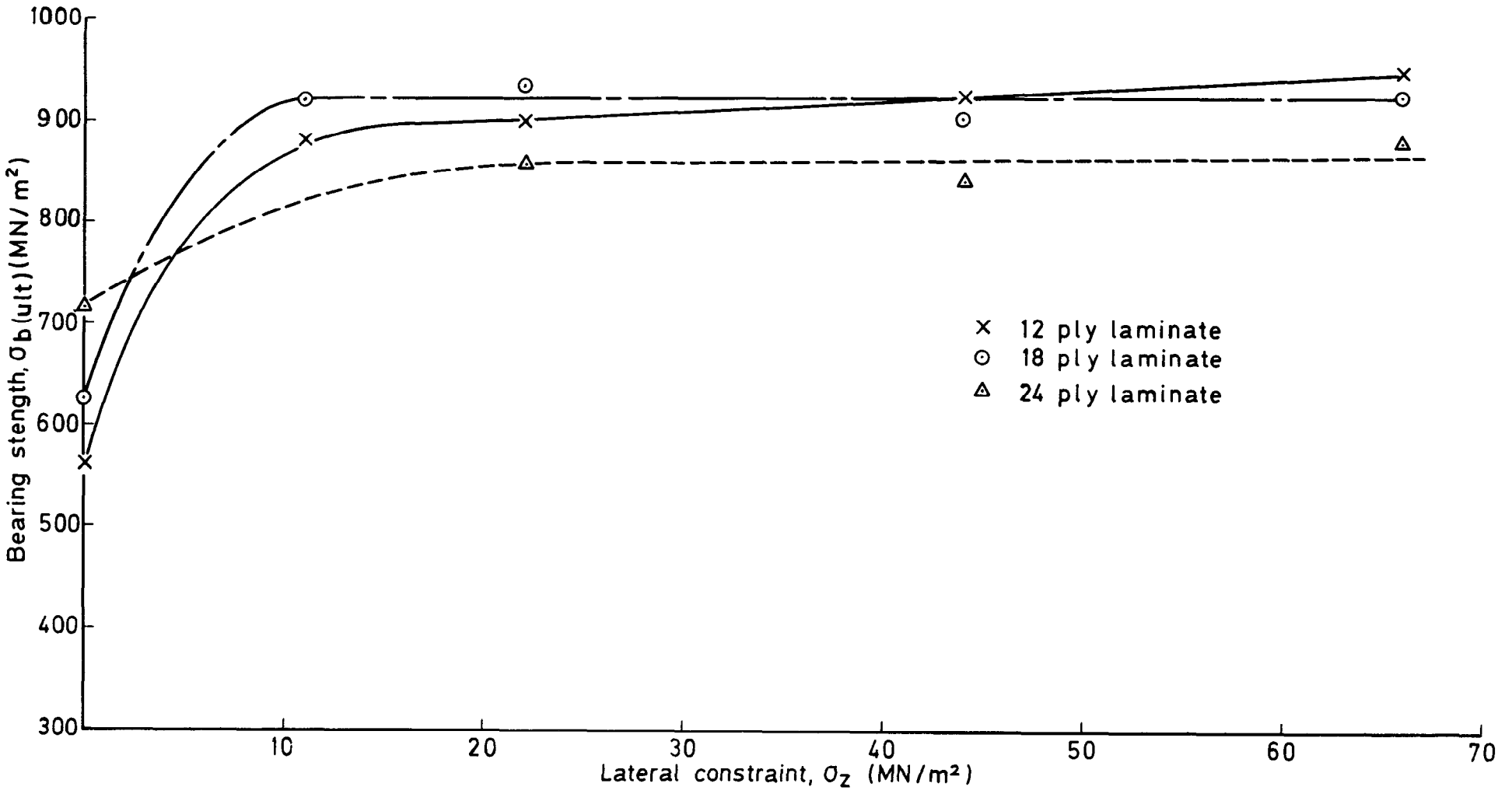

Fig.17 Variation of bearing strength with lateral constraint for various thicknesses of laminate (6·35mm diameter hole, 0° ±45° laminate)

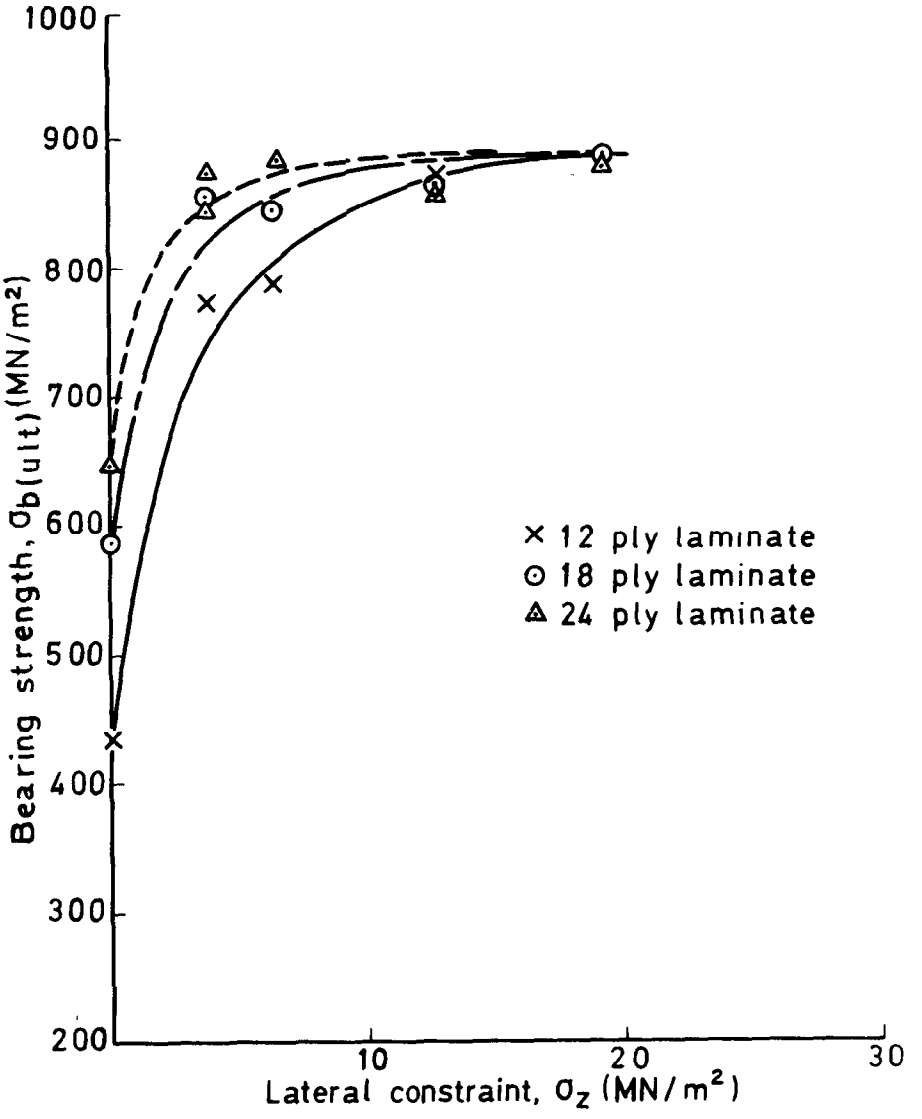

Fig.18 Variation of bearing strength with lateral constraint for various thicknesses of laminate (9·53mm diameter hole, 0° ± 45° laminate)

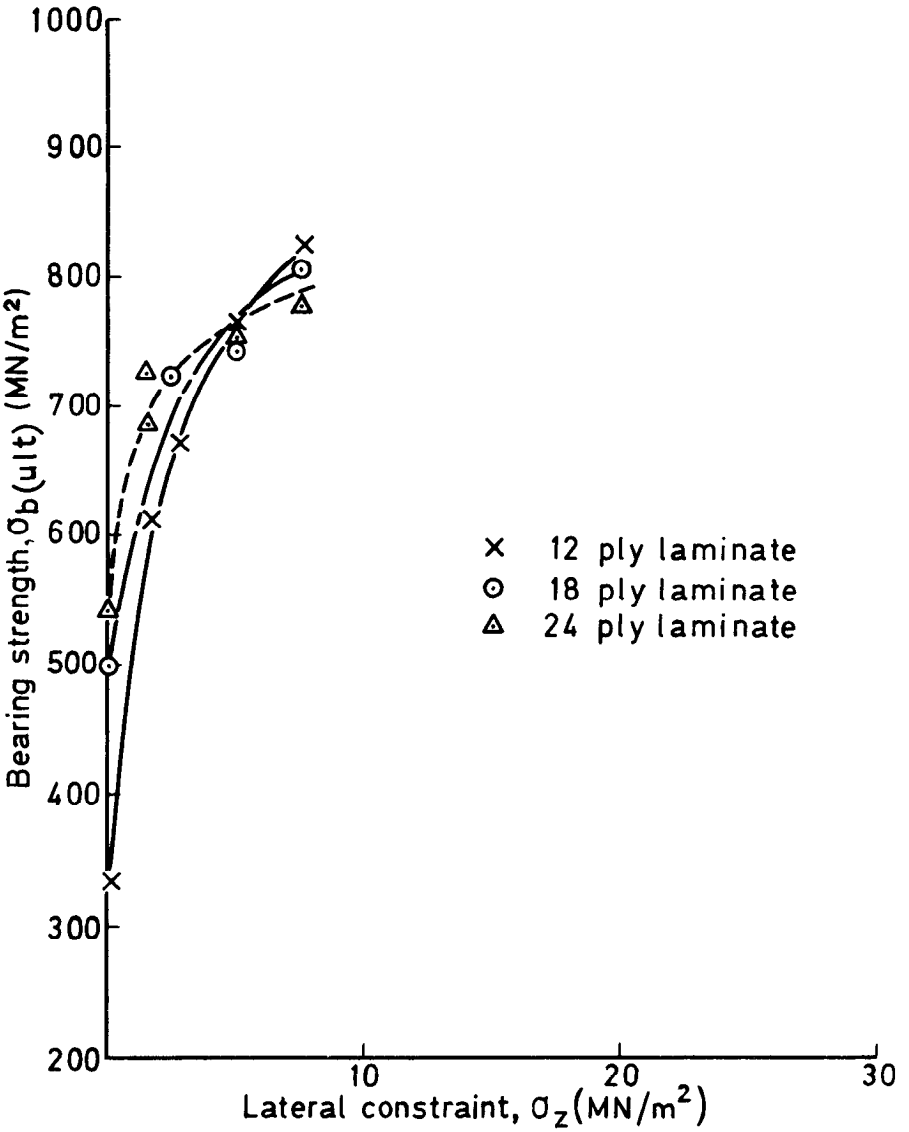

Fig. 19 Variation of bearing strength with lateral constraint for various thicknesses of laminate (12·7mm diameter hole, 0° ±45° laminate)

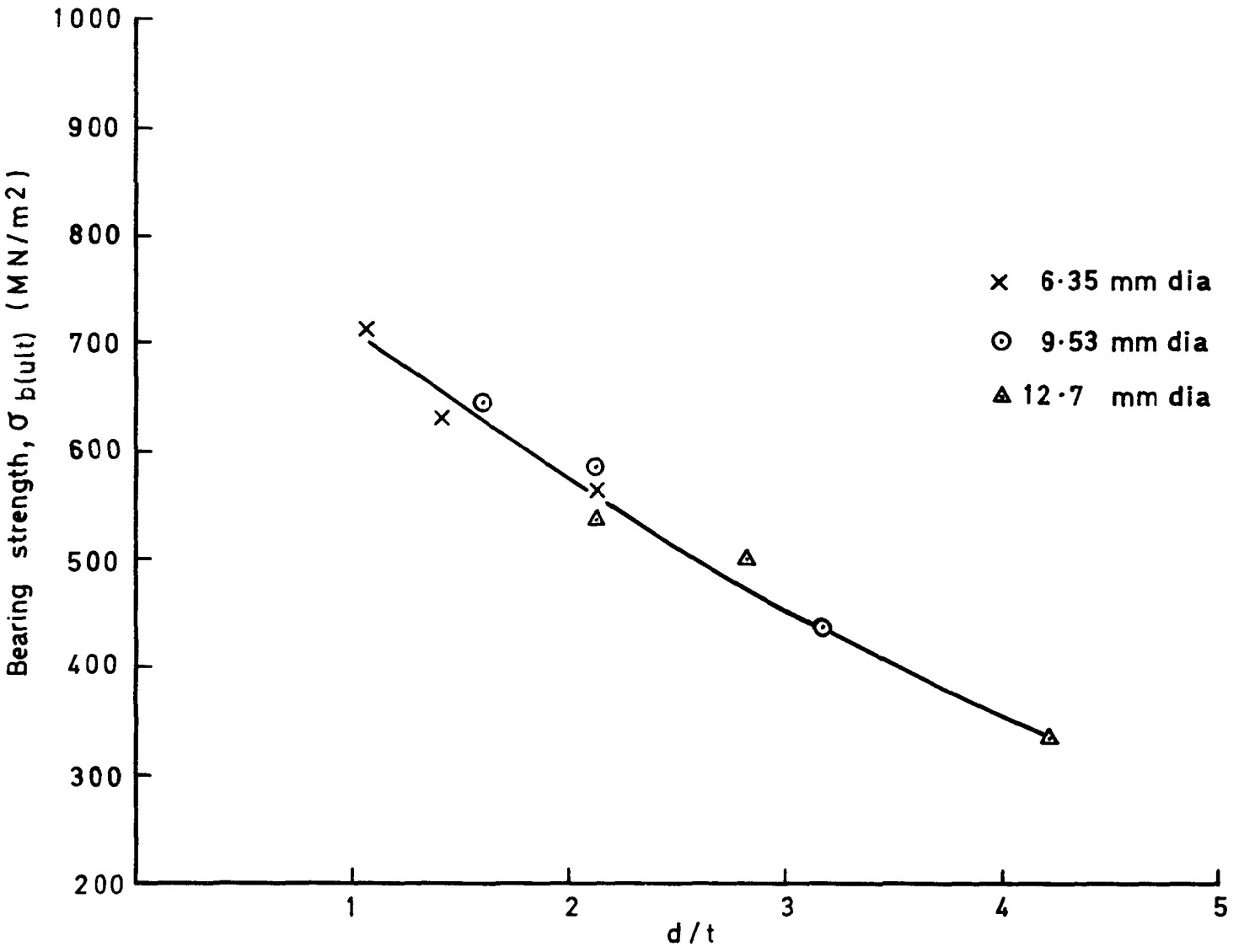

Fig.20 Variation of bearing strength with d/t ratio ($0^\circ \pm 45^\circ$ laminate, without lateral constraint)

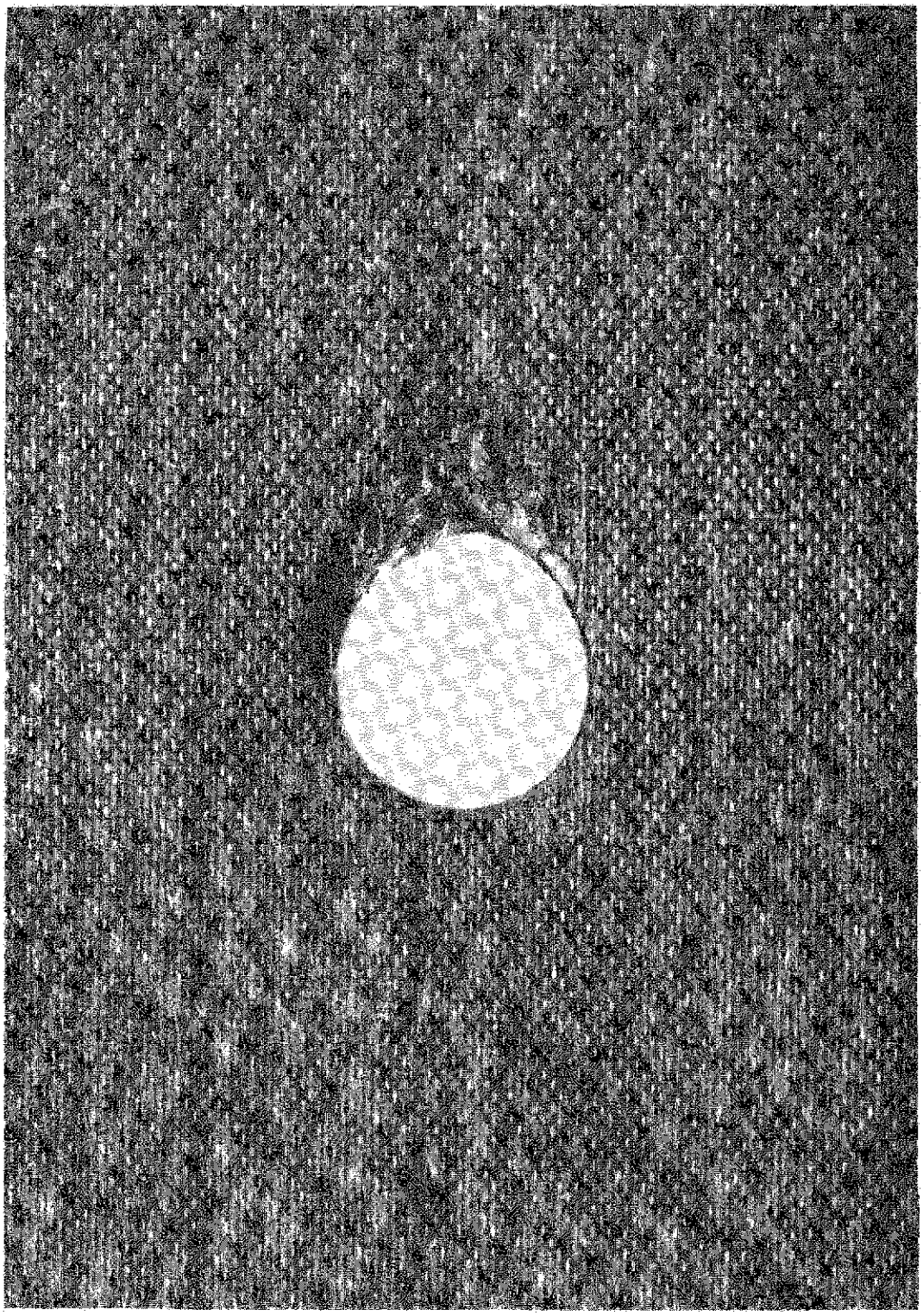

$0^{\circ} \pm 45^{\circ}$ laminate

Fig.21 Bearing failure (without lateral constraint)

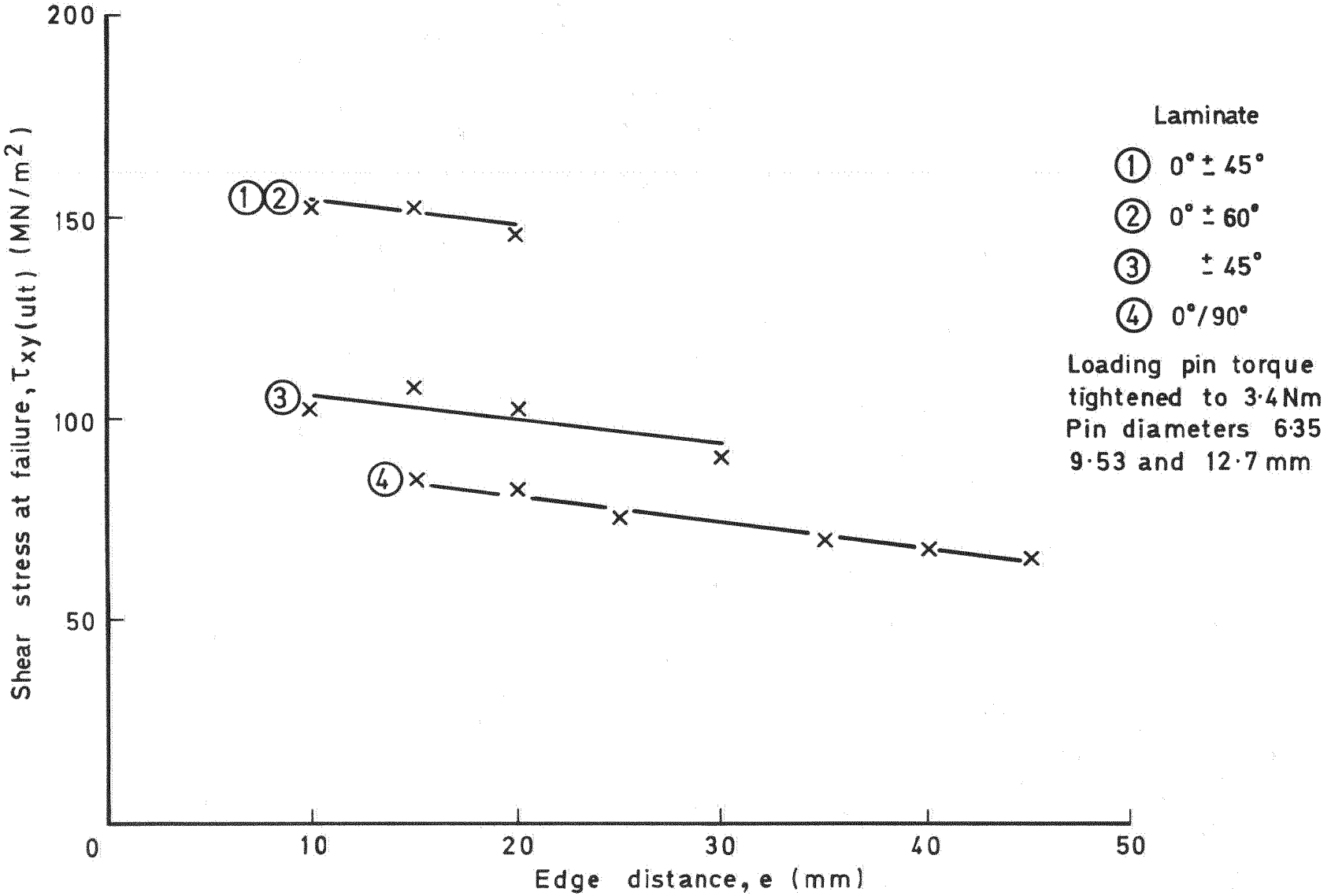

Fig.22 Variation of shear strength with edge distance

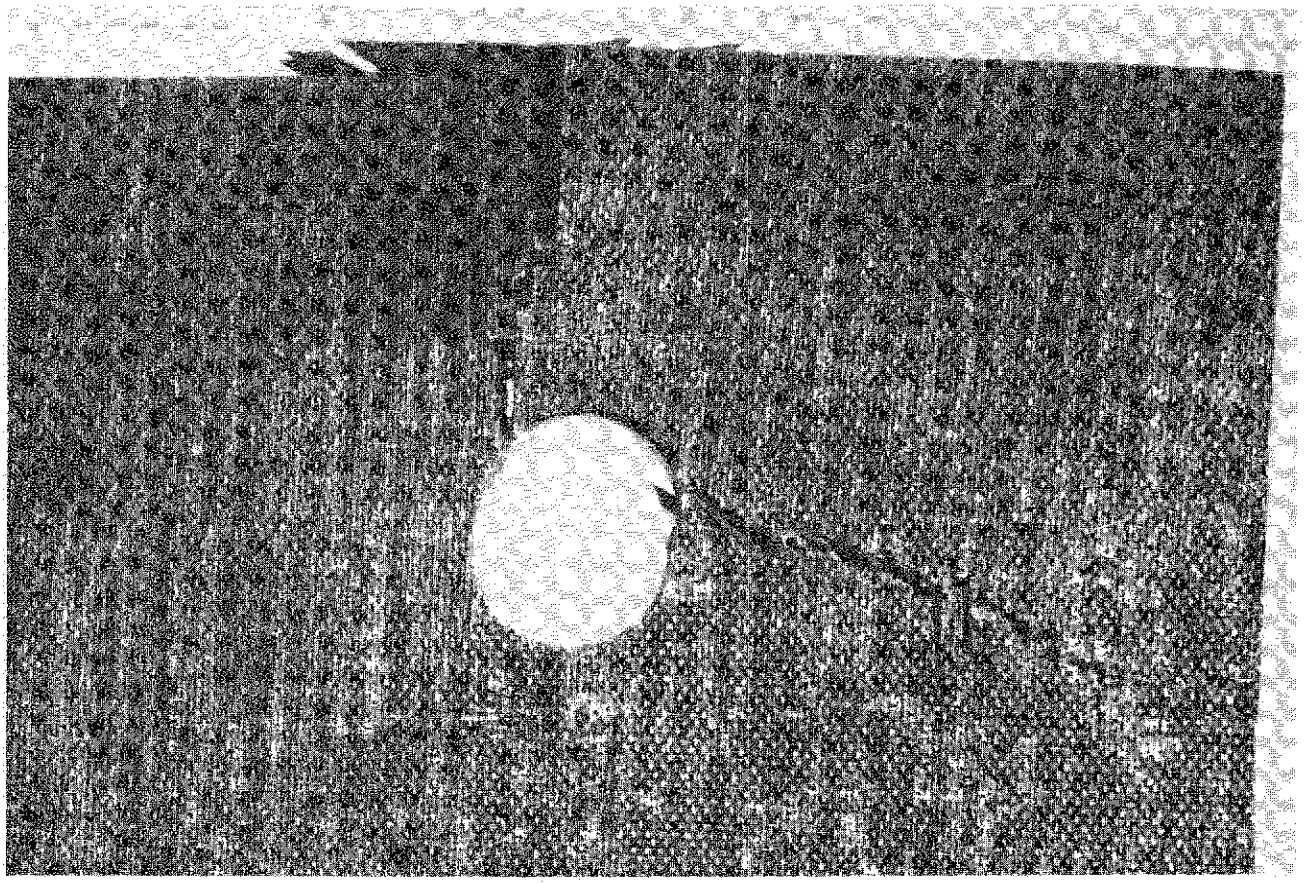

a. $0^{\circ} \pm 45^{\circ}$ laminate

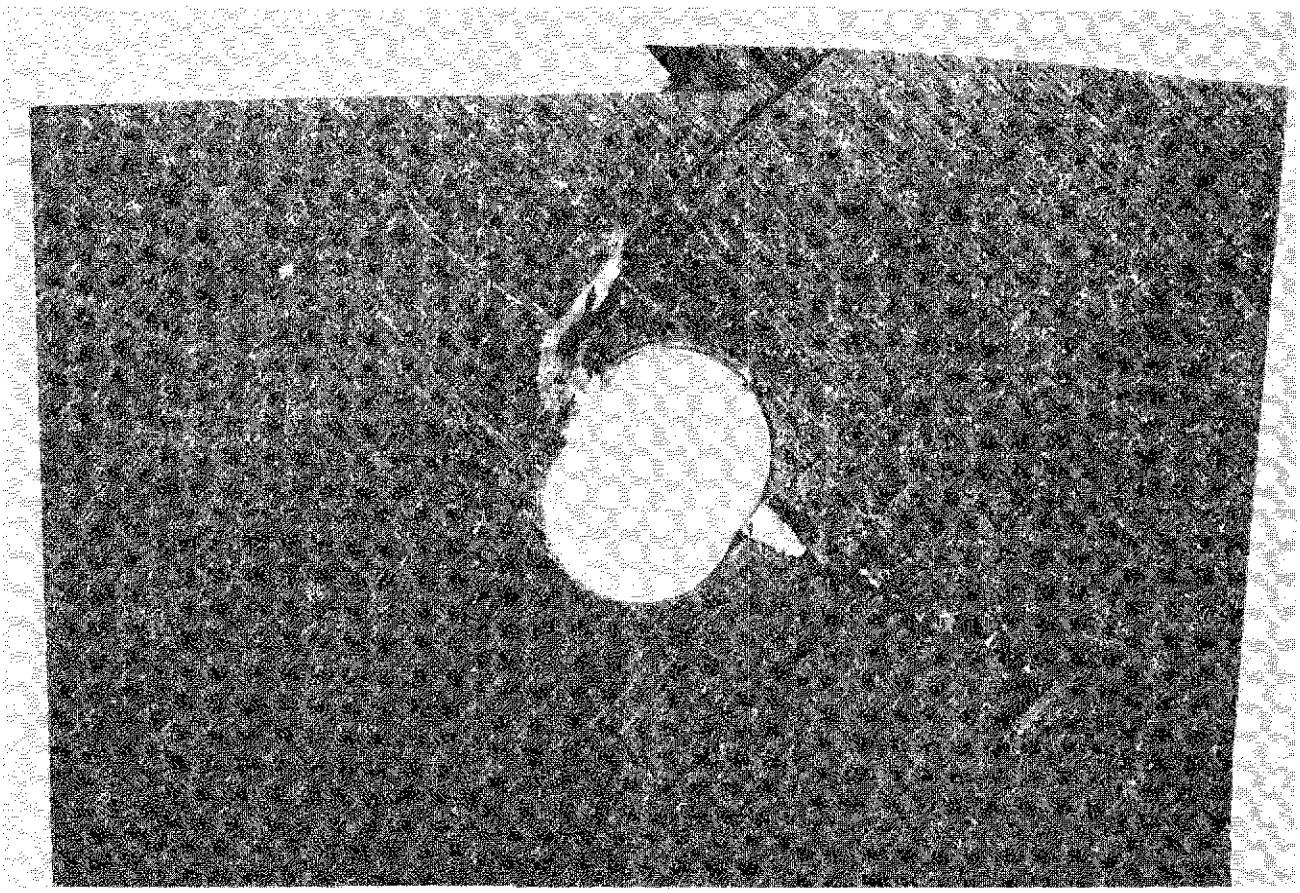

b. $\pm 45^{\circ}$ laminate

Fig.23a & b Shear failures

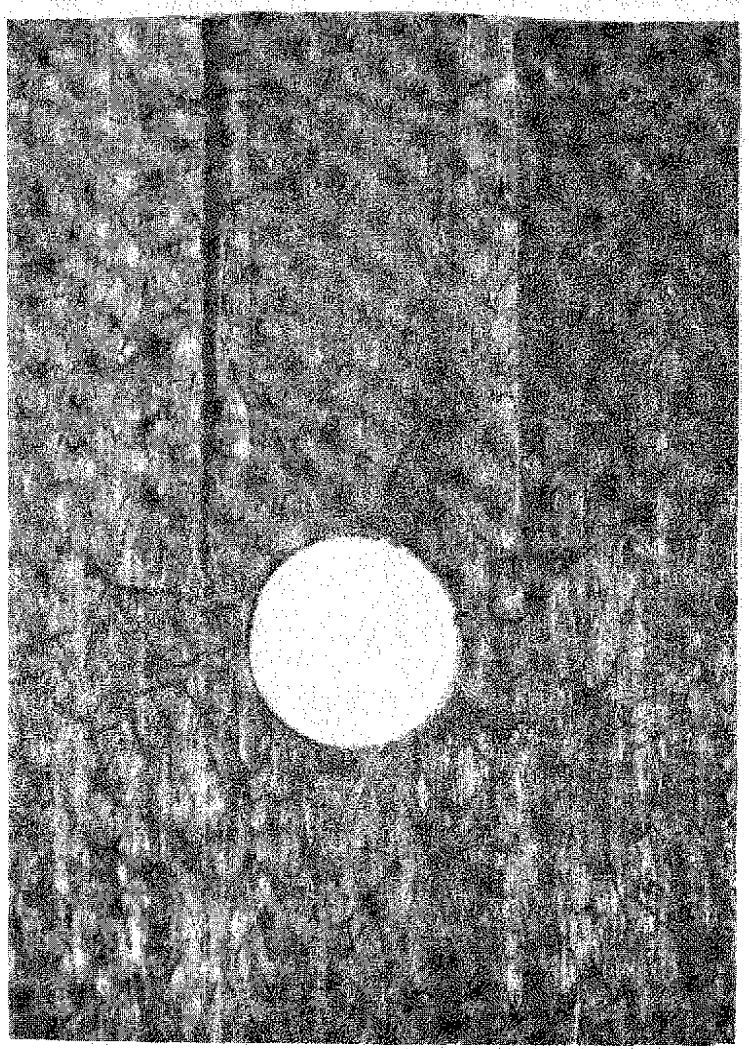

c. $0^{\circ}/90^{\circ}$ laminate

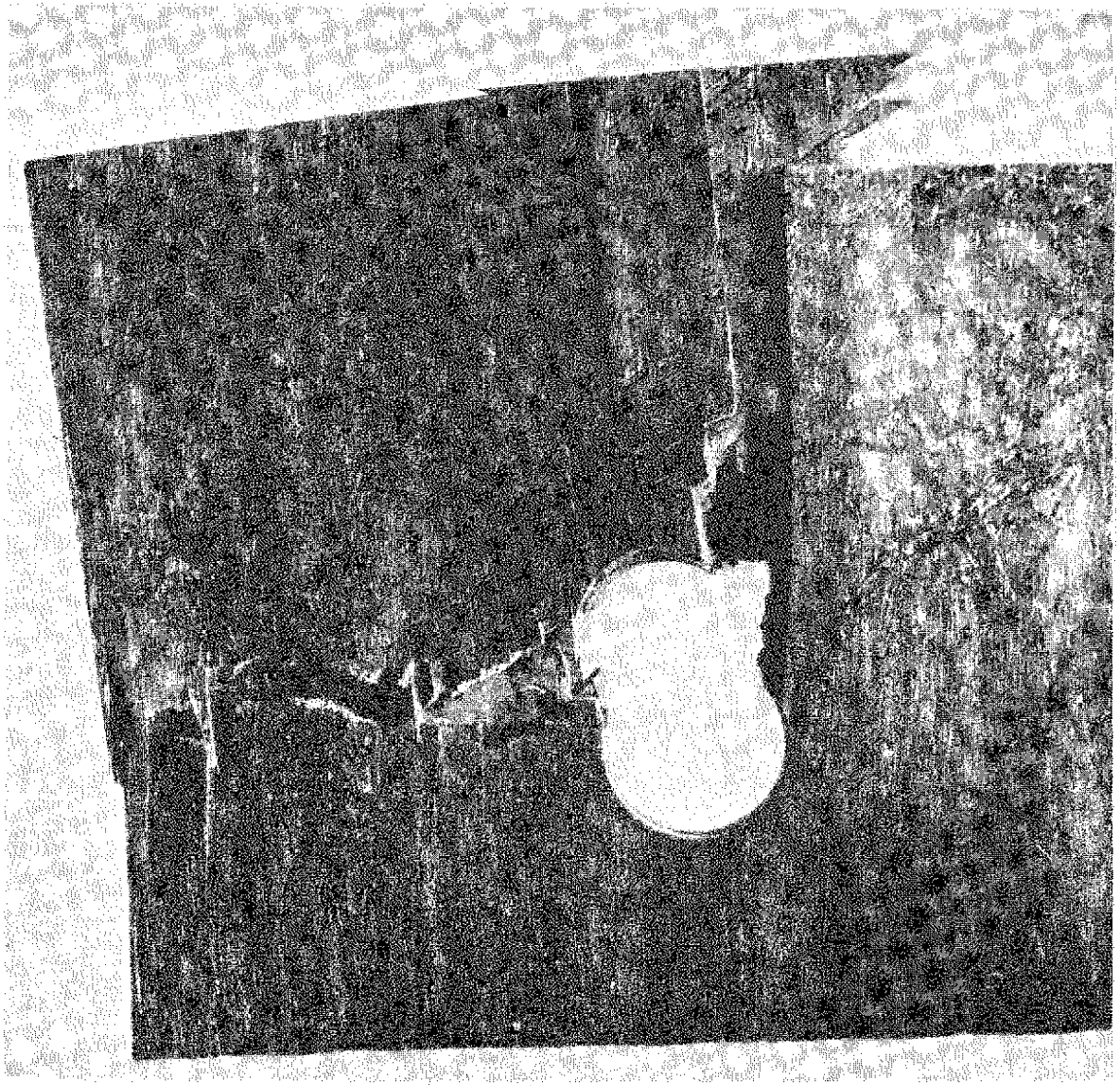

d. $0^{\circ} \pm 60^{\circ}$ laminate

Fig.23c & d Shear failures

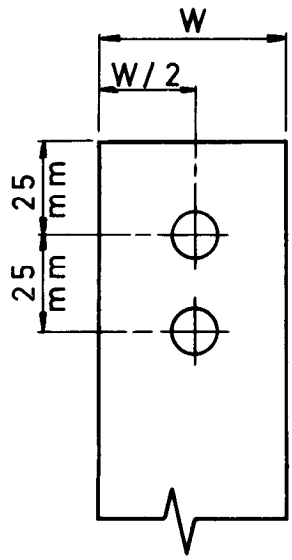

Two holes in tandem

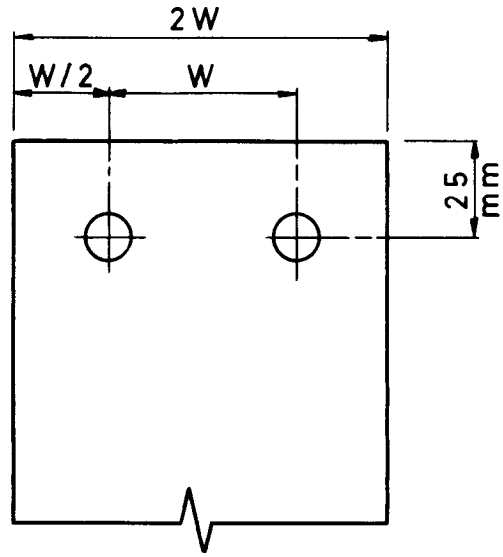

Two holes side-by-side

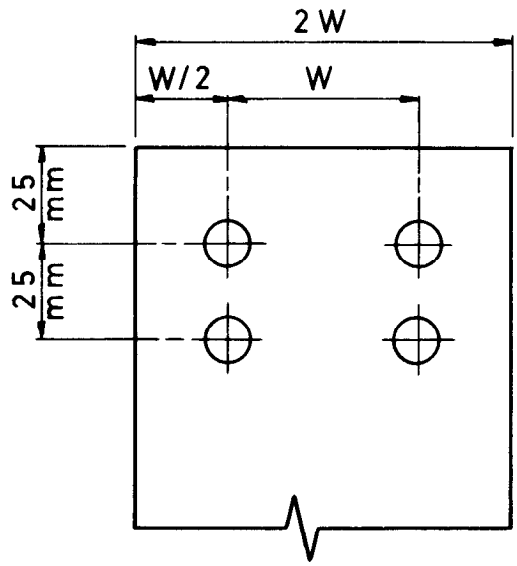

Four hole group
(Two tandem joints side-by-side)

Fig. 24 Hole groupings

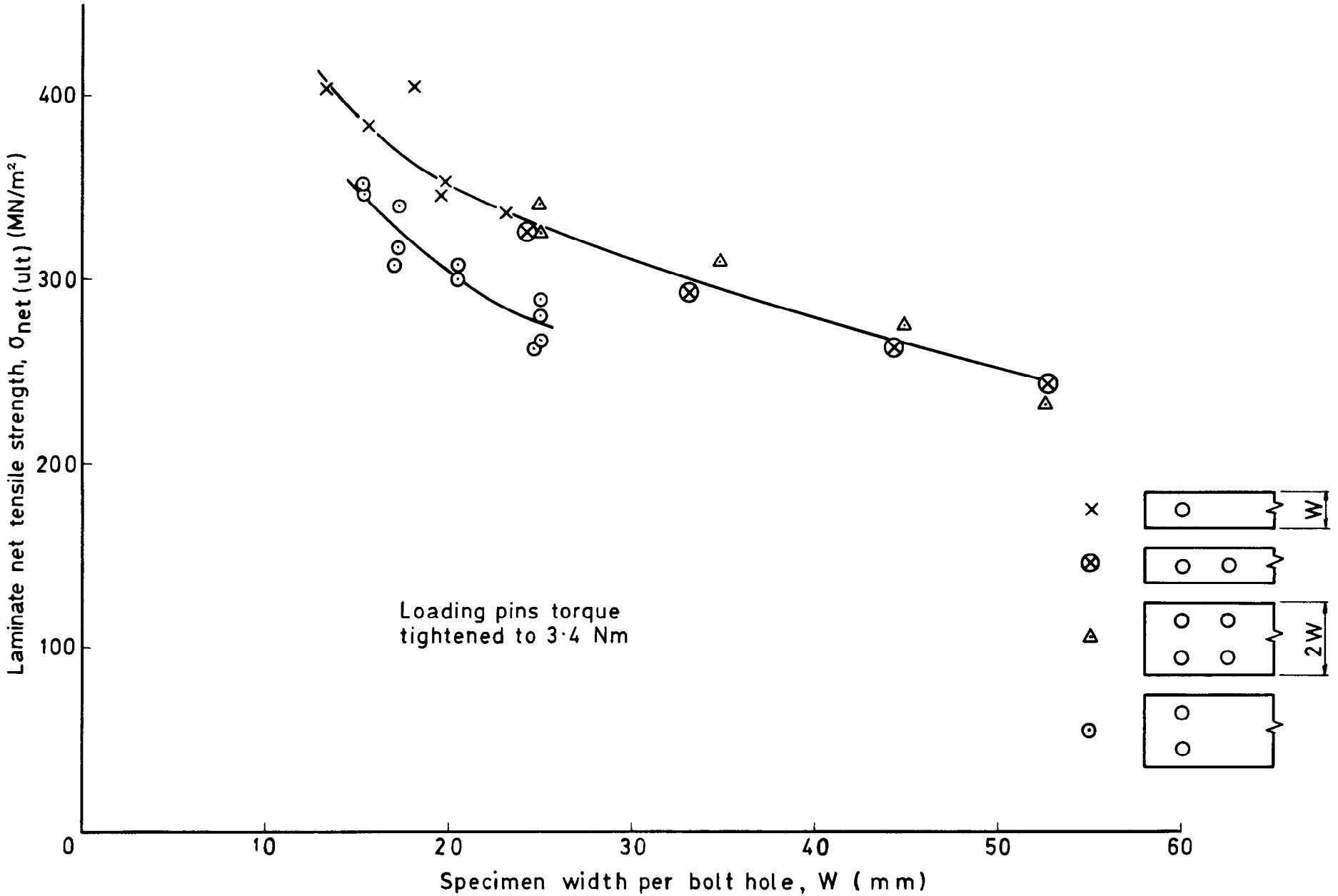

Fig.25 Variation of net tensile strength with specimen width per bolt hole (single and multi-holed specimens, 0° ±45° laminate)

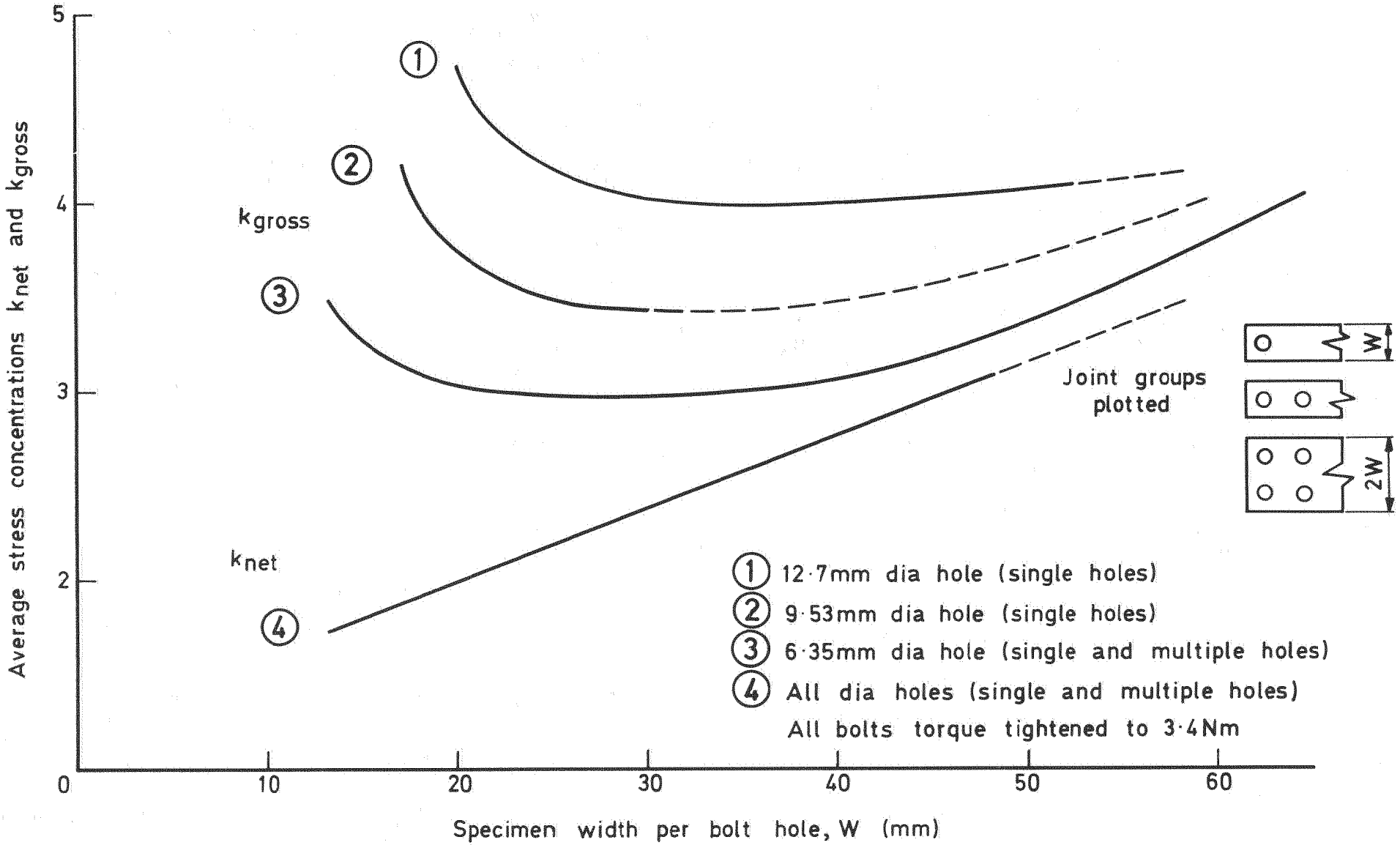

Fig. 26 Average tensile stress concentration factors ($0° \pm 45°$ laminate)

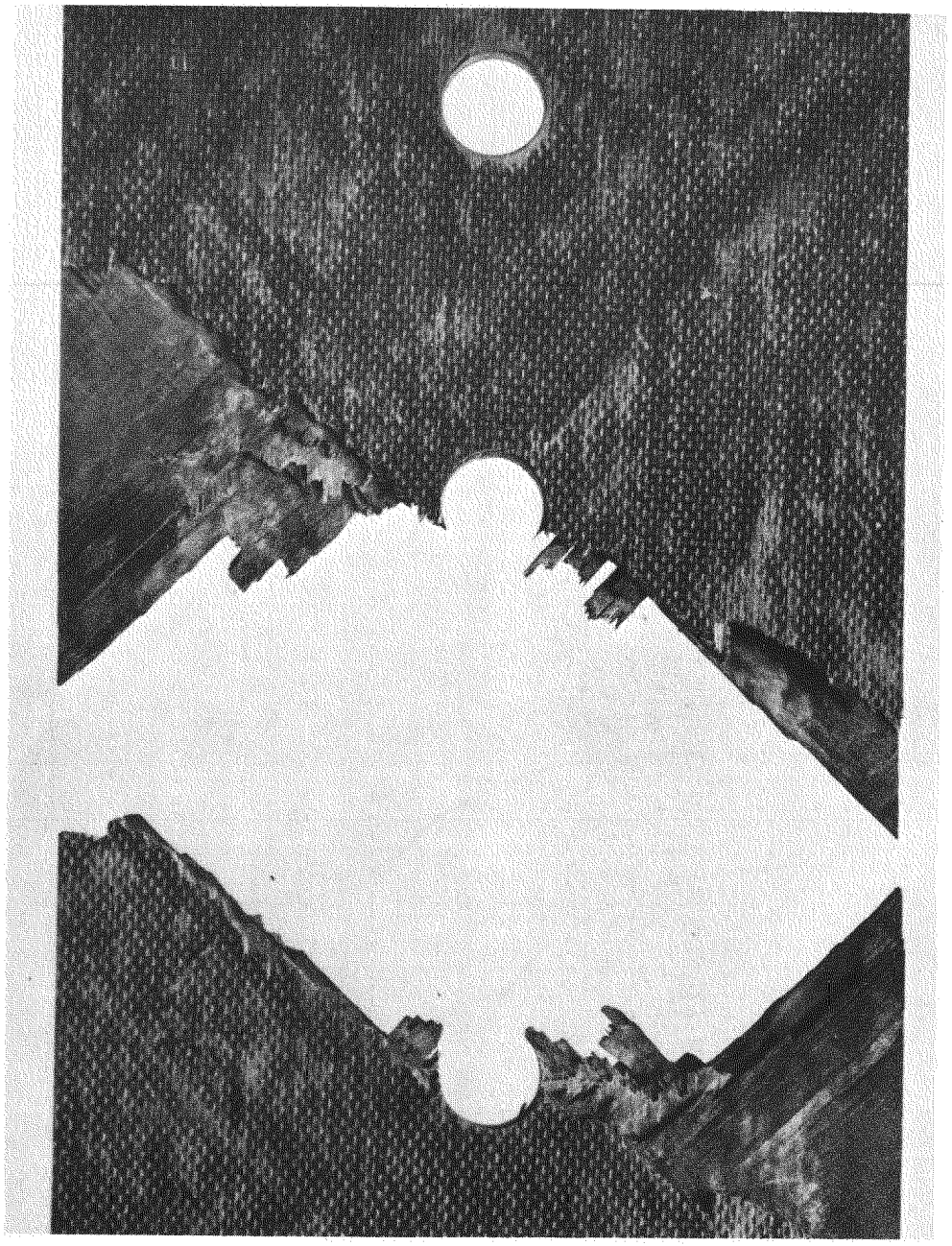

a. Two holes in tandem

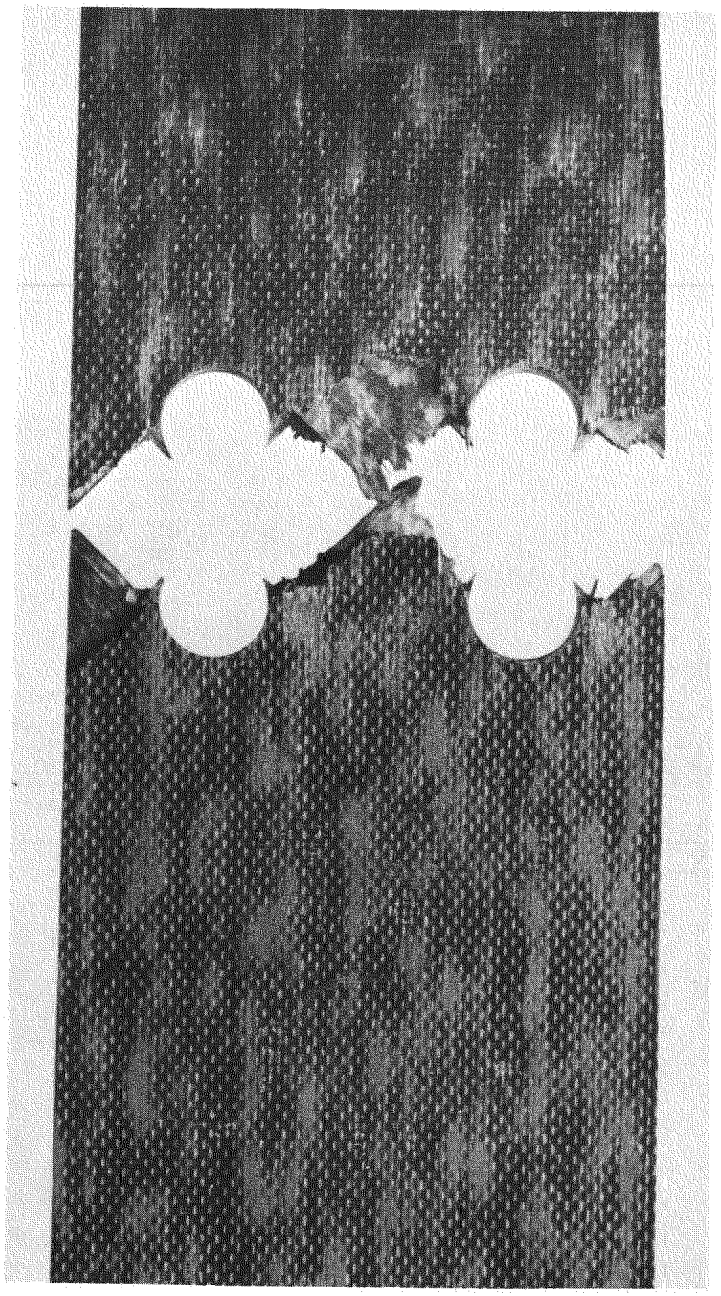

b. Two holes side-by-side

Fig.27a & b Tensile failure of $0^\circ \pm 45^\circ$ laminates

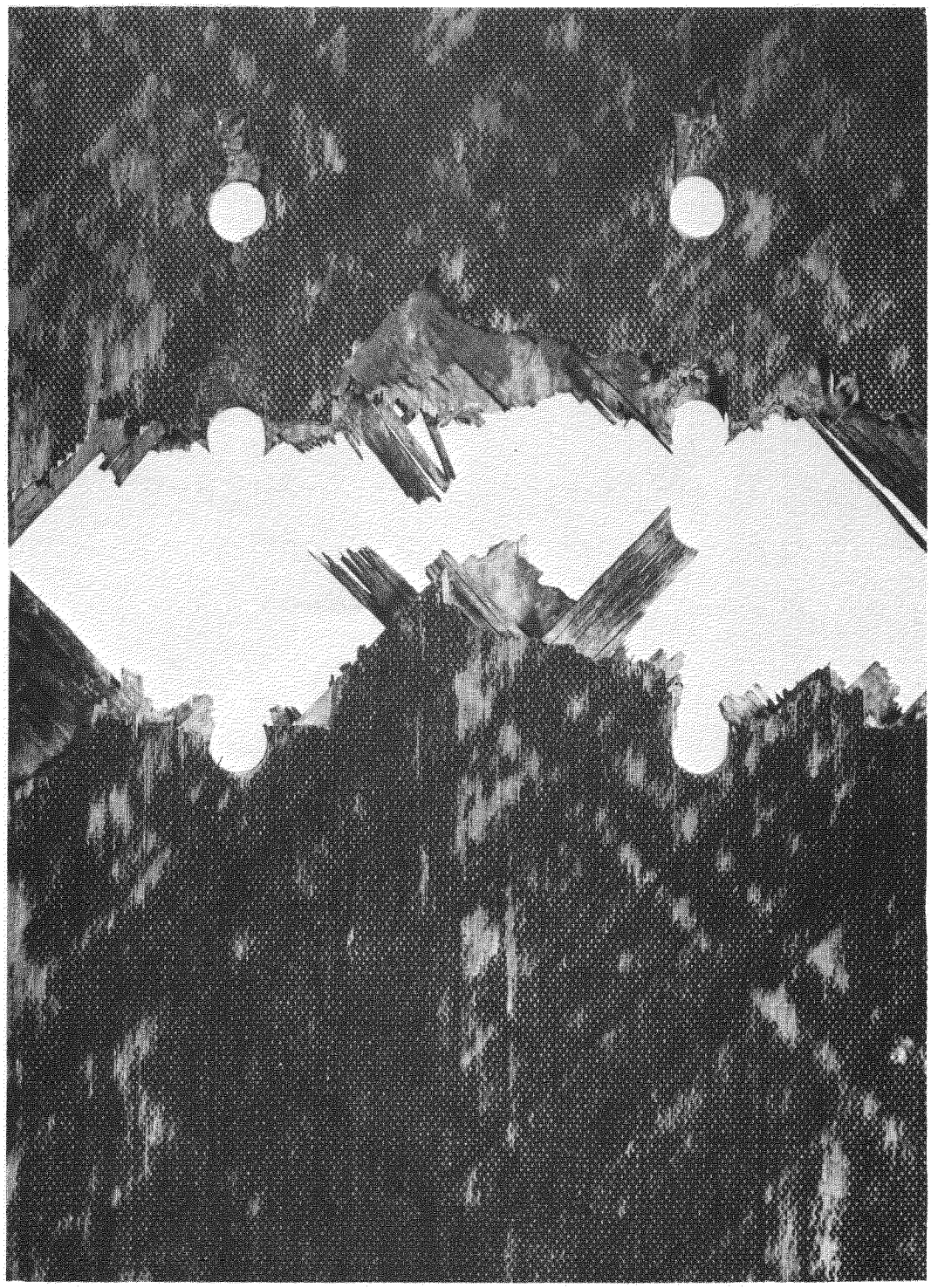

c. Four hole group (two tandem joints side-by-side)

Fig.27c Tensile failure of $0^\circ \pm 45^\circ$ laminates

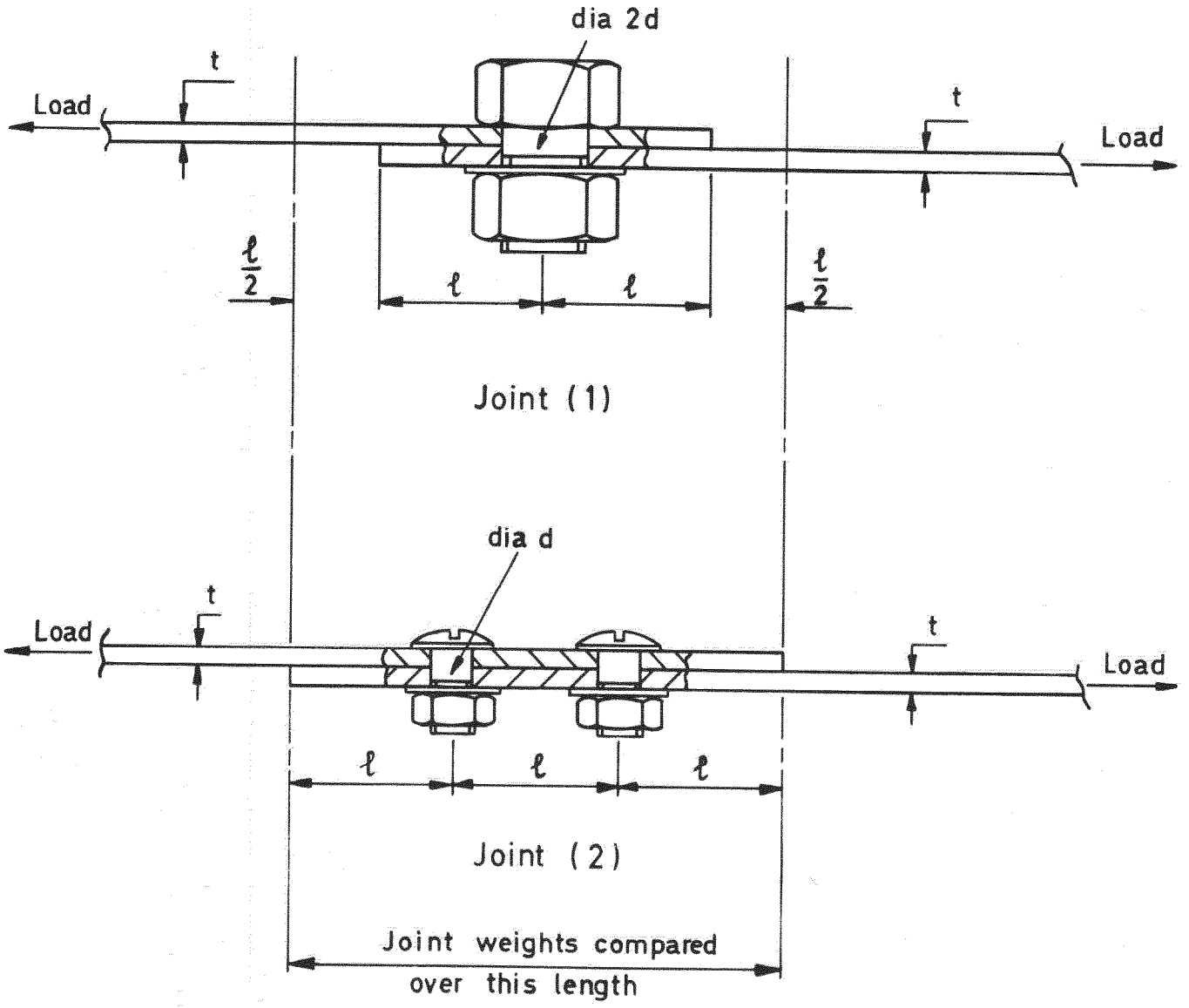

W = 50 mm ℓ = 25 mm t = 3 mm d = 6·35 mm

Fig. 28 Comparison of Joints

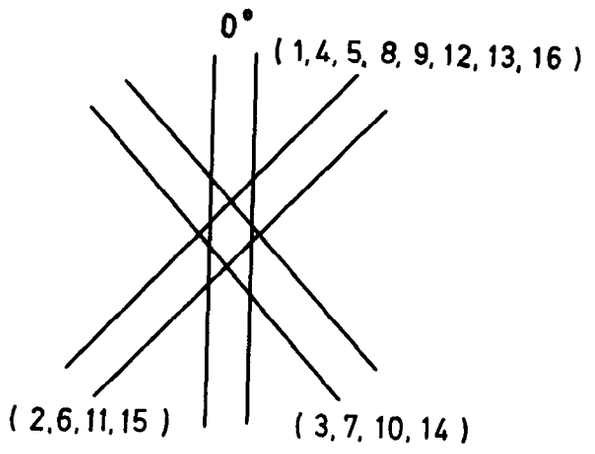

a $\frac{1}{2}$ 0° $\frac{1}{2}$ ± 45°

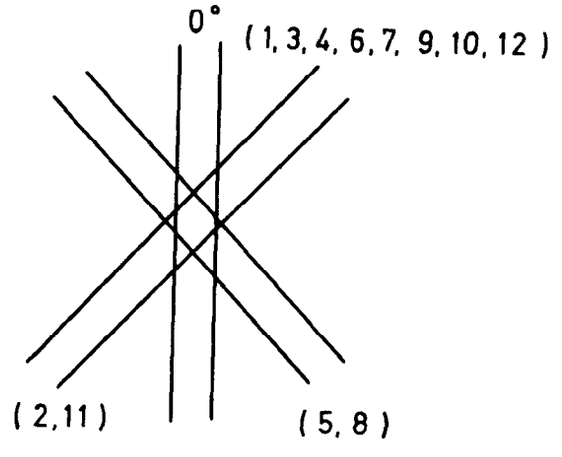

b $\frac{2}{3}$ 0° $\frac{1}{3}$ ± 45°

Fig.29a & b Stacking sequences for 0° ± 45° laminates

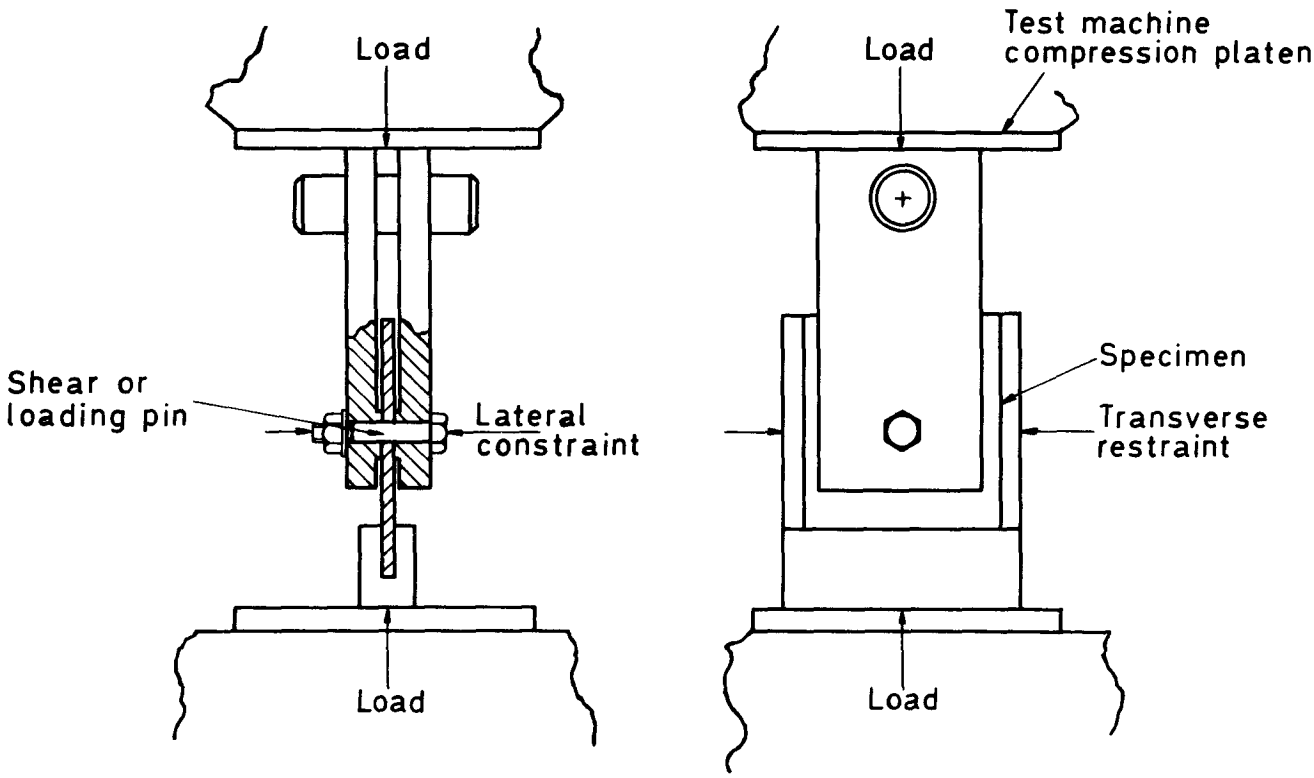

Fig. 30 Loading arrangement of a unidirectional specimen under lateral & transverse restraint

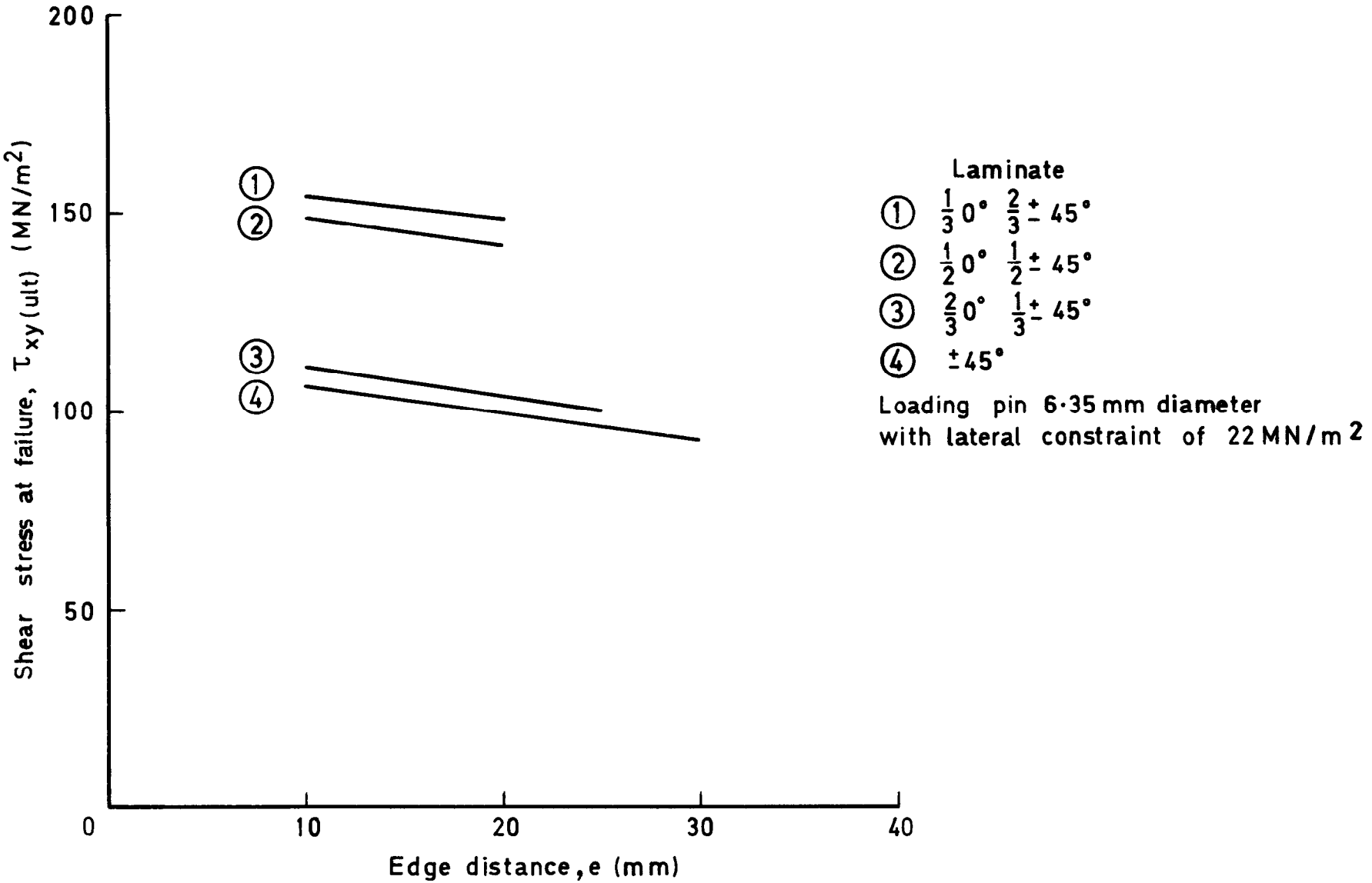

Fig. 31 Variation of shear strength with edge distance (0° ± 45° laminates)

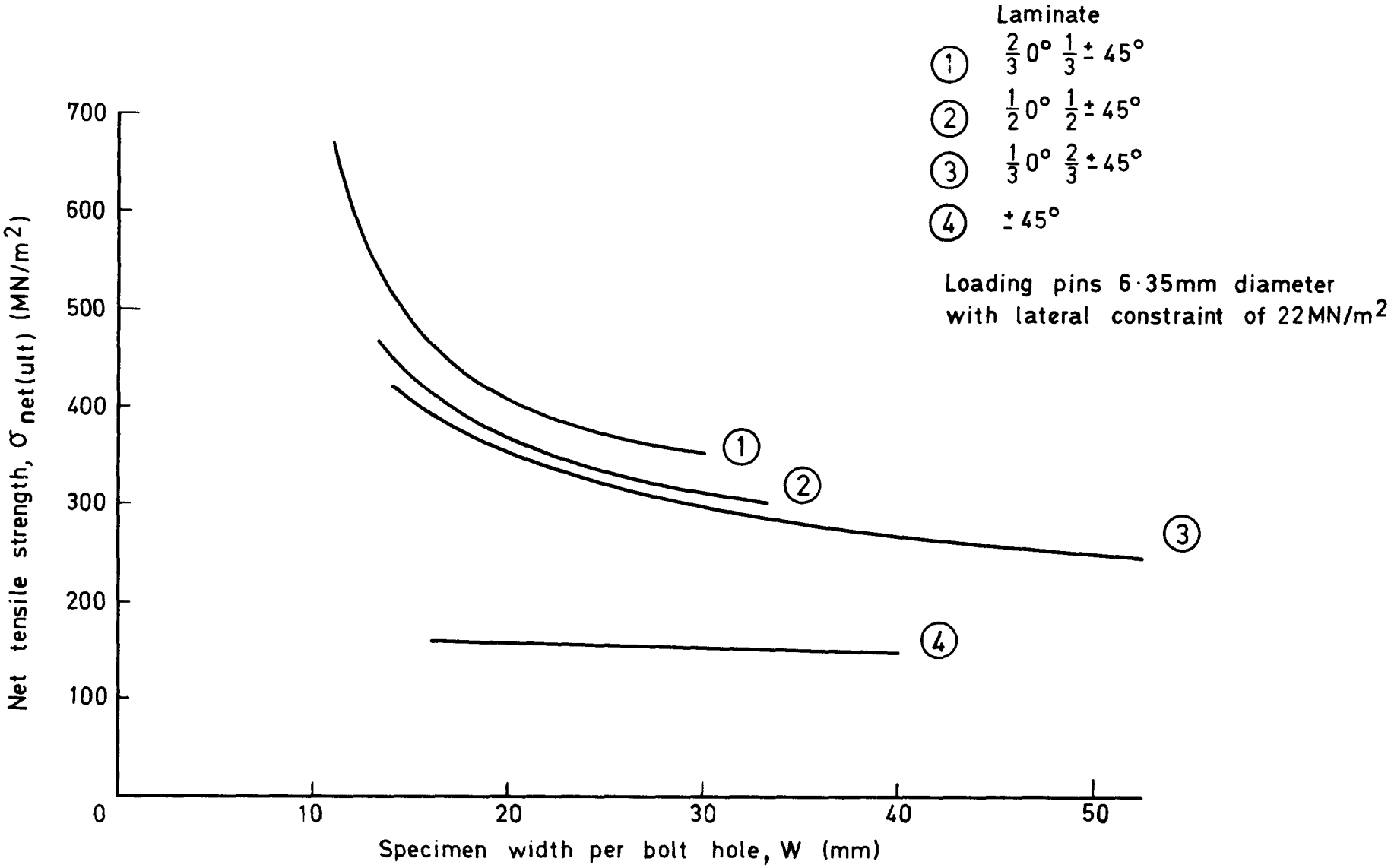

Fig. 32 Variation of net tensile strength with specimen width per bolt hole ($0° \pm 45°$ laminates)

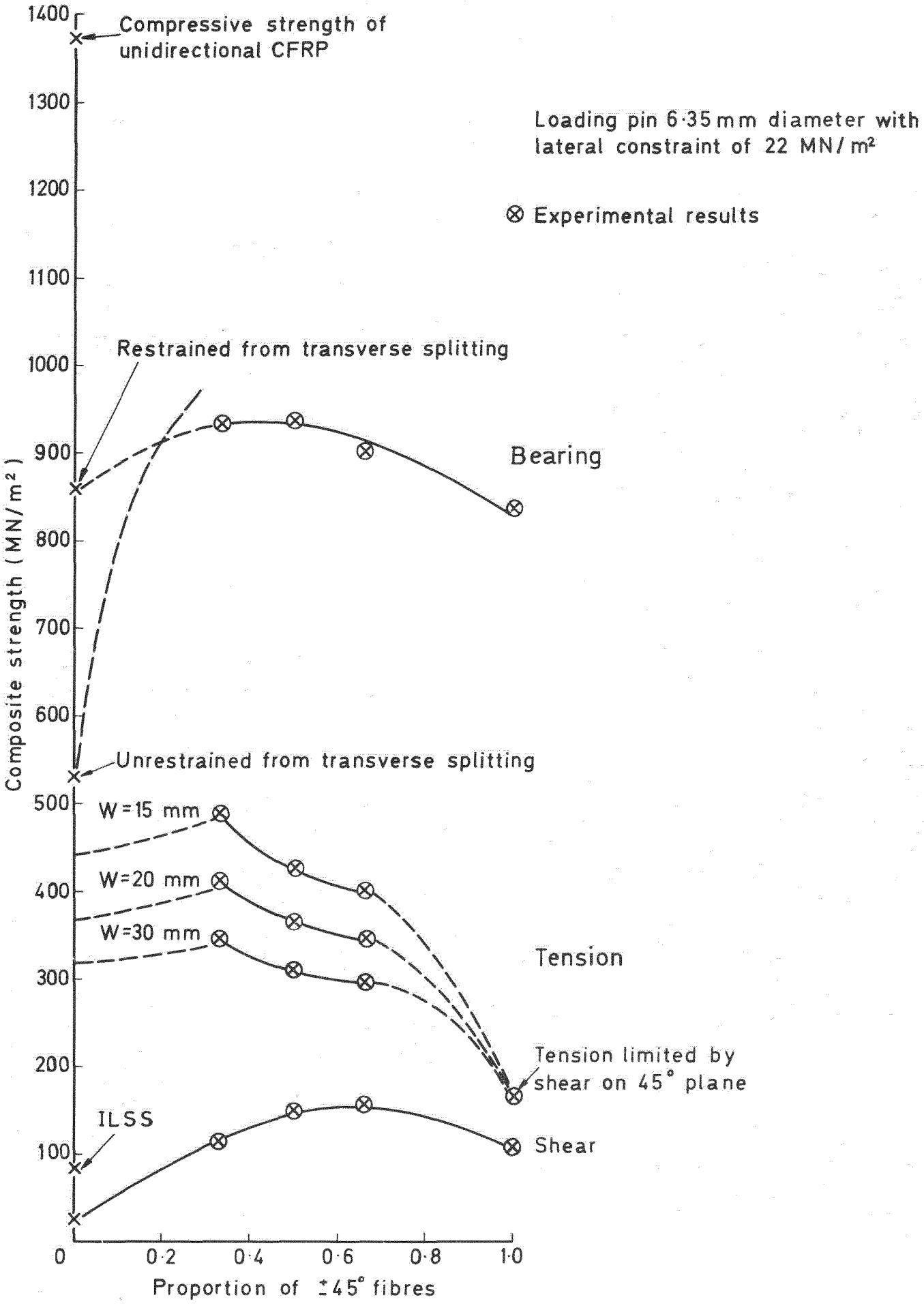

Fig.33 Joint properties of 0° ± 45° laminates containing various proportions of ± 45° fibres

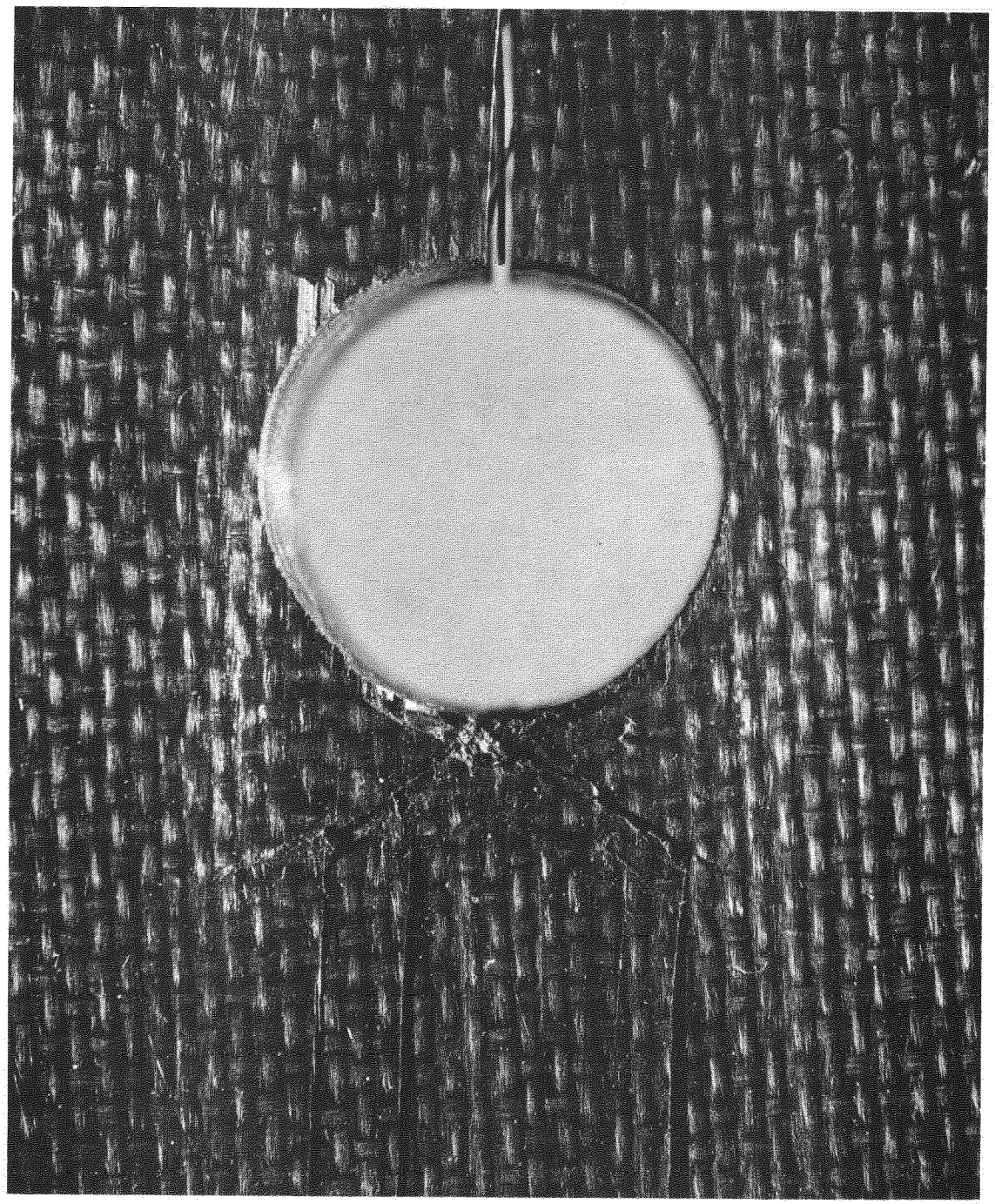

Fig.34 Bearing failure of a unidirectional specimen (transversely restrained)

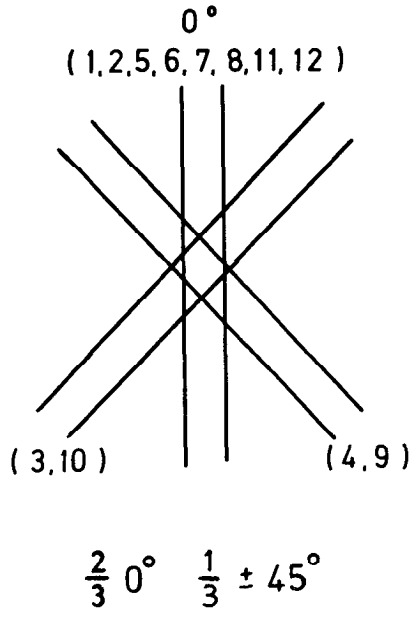

Fig. 35 Stacking sequence for a non-homogeneous $0° \pm 45°$ laminate

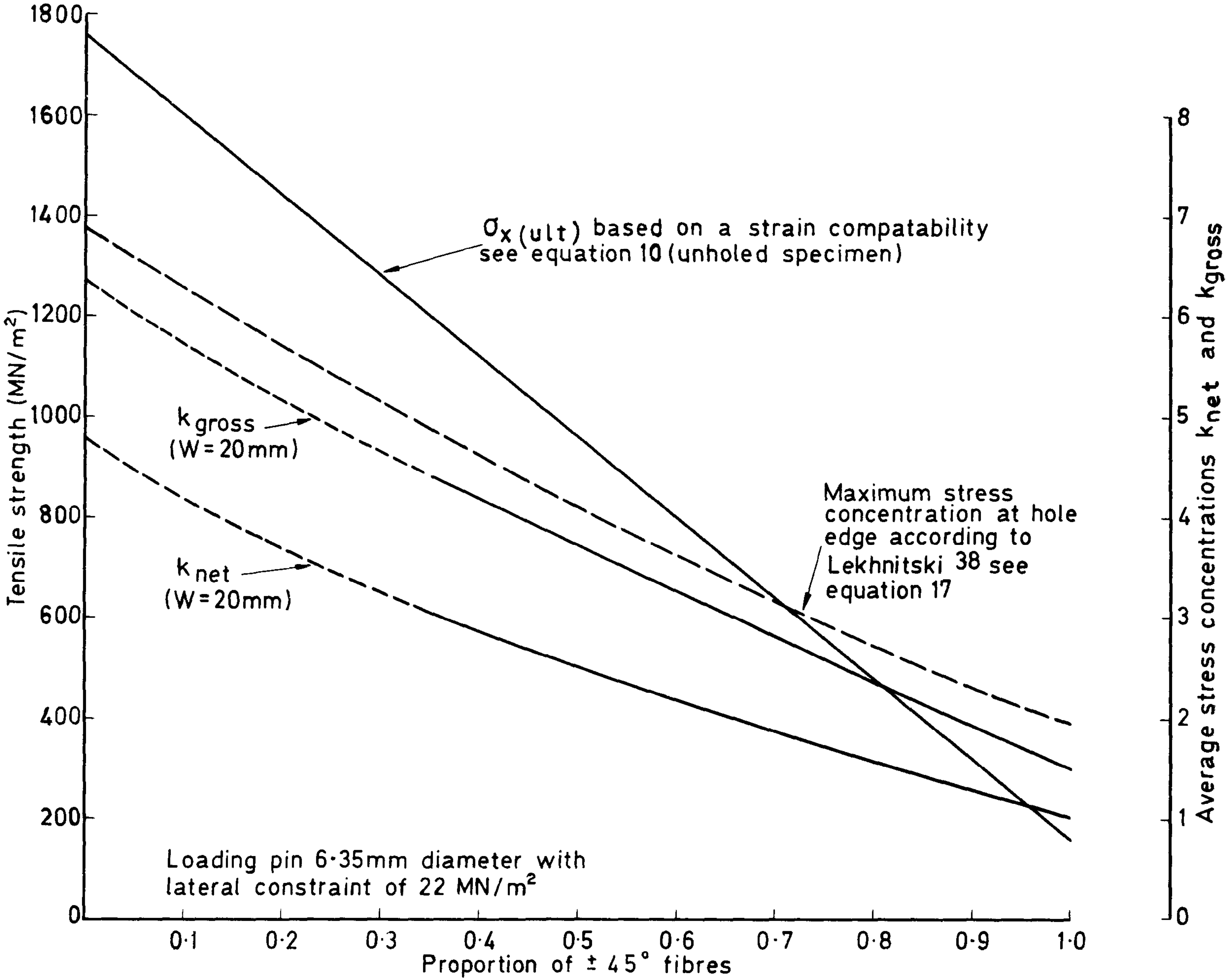

Fig. 36 Variation of tensile strength with proportion of ±45° fibres in 0° ±45° laminates

ARC CP No.1380
December 1975

621.882 :
661.66-426
678.046 :
621-419 :
539.41

Collings, T.A.

THE STRENGTH OF BOLTED JOINTS IN MULTI-DIRECTIONAL CFRP LAMINATES

Tests have been carried out on simple bolted joints in multi-directional CFRP for a range of laminate configurations and hole sizes. For single-hole joints the various modes of failure have been isolated and the corresponding strengths measured; the effects of variables such as ply orientation, laminate thickness and bolt clamping pressure are discussed in the light of the results.

Multi-hole joints have been designed using the single-hole data and test results show that for normal bolt spacings there is little interaction between holes. The results also show that the specific static strengths of these joints can be significantly better than those in conventional materials such as aluminium alloy and steel.

ARC CP No.1380
December 1975

621.882 :
661.66-426 :
678.046 :
621-419 :
539.41

Collings, T.A.

THE STRENGTH OF BOLTED JOINTS IN MULTI-DIRECTIONAL CFRP LAMINATES

Tests have been carried out on simple bolted joints in multi-directional CFRP for a range of laminate configurations and hole sizes. For single-hole joints the various modes of failure have been isolated and the corresponding strengths measured; the effects of variables such as ply orientation, laminate thickness and bolt clamping pressure are discussed in the light of the results.

Multi-hole joints have been designed using the single-hole data and test results show that for normal bolt spacings there is little interaction between holes. The results also show that the specific static strengths of these joints can be significantly better than those in conventional materials such as aluminium alloy and steel.

ARC CP No.1380
December 1975

621.882 :
661.66-426 :
678.046 :
621-419 :
539.41

Collings, T.A.

THE STRENGTH OF BOLTED JOINTS IN MULTI-DIRECTIONAL CFRP LAMINATES

Tests have been carried out on simple bolted joints in multi-directional CFRP for a range of laminate configurations and hole sizes. For single-hole joints the various modes of failure have been isolated and the corresponding strengths measured; the effects of variables such as ply orientation, laminate thickness and bolt clamping pressure are discussed in the light of the results.

Multi-hole joints have been designed using the single-hole data and test results show that for normal bolt spacings there is little interaction between holes. The results also show that the specific static strengths of these joints can be significantly better than those in conventional materials such as aluminium alloy and steel.

ARC CP No.1380
December 1975

621.882 :
661.66-426 :
678.046 :
621-419 :
539.41

Collings, T.A.

THE STRENGTH OF BOLTED JOINTS IN MULTI-DIRECTIONAL CFRP LAMINATES

Tests have been carried out on simple bolted joints in multi-directional CFRP for a range of laminate configurations and hole sizes. For single-hole joints the various modes of failure have been isolated and the corresponding strengths measured; the effects of variables such as ply orientation, laminate thickness and bolt clamping pressure are discussed in the light of the results.

Multi-hole joints have been designed using the single-hole data and test results show that for normal bolt spacings there is little interaction between holes. The results also show that the specific static strengths of these joints can be significantly better than those in conventional materials such as aluminium alloy and steel.

DETACHABLE ABSTRACT CARDS

DETACHABLE ABSTRACT CARDS

1977

Published by
HER MAJESTY'S STATIONERY OFFICE

Government Bookshops
49 High Holborn, London WC1V 6HB
13a Castle Street, Edinburgh EH2 3AR
41 The Hayes, Cardiff CF1 1JW
Brazennose Street, Manchester M60 8AS
Southey House, Wine Street, Bristol BS1 2BQ
258 Broad Street, Birmingham B1 2HE
80 Chichester Street, Belfast BT1 4JY
Government Publications are also available through booksellers

C.P. No. 1380

ISBN 011 471126 7